GEOLOGICA CARPATHICA, APRIL 2020, 71, 2, 113–133 https://doi.org/10.31577/GeolCarp.71.2.2

Hydrothermal mineralisation of the Tatric Superunit (Western Carpathians, Slovakia): II. Geochronology and timing of mineralisations in the Nízke Tatry Mts.

JURAJ MAJZLAN[1,✉], MARTIN CHOVAN[2], STEFAN KIEFER[1], AXEL GERDES[3], MILAN KOHÚT[4], PAVOL SIMAN[4], PATRIK KONEČNÝ[5], MARTIN ŠTEVKO[6], FRITZ FINGER[7], MICHAEL WAITZINGER[7], ADRIAN BIROŇ[8], JARMILA LUPTÁKOVÁ[8], LUKÁŠ ACKERMAN[9,10] and JOHN M. HORA[10]

[1]Institute of Geosciences, Friedrich-Schiller University, Burgweg 11, D–07749 Jena, Germany; ✉Juraj.Majzlan@uni-jena.de
[2]Department of Mineralogy and Petrology, Comenius University, Mlynská dolina G, 842 15 Bratislava, Slovakia
[3]Department of Geosciences, Goethe University, Altenhöferallee 1, D-60438 Frankfurt am Main, Germany
[4]Earth Science Institute, Slovak Academy of Sciences, Dúbravská cesta 9, P.O. Box 106, 840 05 Bratislava, Slovakia
[5]State Geological Institute of Dionýz Štúr, Mlynská dolina 1, 817 04, Bratislava, Slovakia
[6]Department of Mineralogy and Petrology, National Museum, Cirkusová 1711340, 193 00 Praha 9, Czech Republic
[7]Department of Chemistry and Physics of Materials, University of Salzburg, Jakob-Haringer-Strasse 2a, A-5020 Salzburg Austria
[8]Earth Science Institute, Slovak Academy of Sciences, Ďumbierska 1, 974 11 Banská Bystrica, Slovakia
[9]Institute of Geology of the Czech Academy of Sciences, Rozvojová 269, Prague 6, 165 00, Czech Republic
[10]Czech Geological Survey, Geologická 6, Prague 5, 152 00, Czech Republic

(Manuscript received October 16, 2019; accepted in revised form March 19, 2020; Associated Editor: Peter Koděra)

Abstract: Ore mineralisations from the Nízke Tatry Mts., assigned to a number of mineralisation stages, were dated in this work by U/Pb analysis by laser ablation–sector field–inductively coupled plasma–mass spectrometry (LA–SF–ICP–MS), Re/Os, chemical Th/U/total Pb isochron method (CHIME), and U–total Pb methods. The samples originated mostly from the large Dúbrava deposit, with additional samples from Magurka, Rišianka, Soviansko, and Malé Železné deposits and occurrences. Additional, mostly unpublished Re/Os, K/Ar, and Ar/Ar data are also considered and discussed. Uraninite from a granite pegmatite and molybdenite from quartz veinlets gave ages of 343±1 and ≈351 Ma, respectively, comparable to the ages of the host rocks. The previously published K/Ar datum on biotite from the scheelite stage (330±5 Ma) is interpreted as a cooling age and its relation to the ore mineralisation is not clear. The arsenopyrite–pyrite–gold stage was dated, although only at a single sample, to 320±8 Ma. The ages for the samples of the stibnite–sphalerite–Pb–Sb-sulfosalts stage scatter also around this date, showing that these mineralisations are late Variscan. It could be assumed that this stage formed during the life span of a fluid circulation system and the later precipitation of stibnite and sulfosalts is simply owing to the temperature dependence of Sb solubility in the fluids. Scattered K/Ar data on illite document the Jurassic continental rifting but seem to be linked to none of the hydrothermal stages. The dolomite–baryte–tetrahedrite stage formed during the post-rift thermal relaxation of the Tatric basement, with ages varying between 156±13 and 128±4 Ma. The quartz–tourmaline stage, devoid of ore minerals, formed during the mid-Cretaceous Alpine metamorphism, with the scattered data averaging to ≈100 Ma. The following compression of the Tatric and Veporic complexes is reflected in sparse U/Pb carbonate ages (72 Ma) and remobilisation of uranium mineralisation (70 Ma). The constraints on the age of the quartz–Cu-sulfide and galena–sphalerite stages are insufficient but their formation could be perhaps placed into uppermost Cretaceous. The vein carbonates were remobilised at 17–31 Ma, with most ages clustering around 24 Ma, related to the burial of parts of the Tatric basement under the Central Carpathian Paleogene Basin. This work documents many episodes of Variscan and Alpine hydrothermal activity that can be linked to the tectonothermal evolution of the Western Carpathians.

Keywords: Mineralisation stages, Re/Os, U/Pb, U/Th/Pb, Ar/Ar dating, Variscan ores, Alpine ores.

Introduction

The area of the Central Western Carpathians (CWC) has been endowed with a number of larger and smaller ore deposits and occurrences, mined from prehistoric times until the early 1990s. The CWC are a part of an Alpine orogenic belt (Plašienka 2018) separated from the Outer Western Carpathians by a thin, 600 km long suture zone (the Pieniny Klippen belt) and plunging under the Tertiary volcanic rocks and the Cenozoic–Neogene and Quaternary sediments of the Pannonian Basin. The CWC consist of the Tatric, Veporic, and Gemeric Superunits; all of them contain the Variscan crystalline basement composed by the metamorphic and magmatic rocks, and their autochtonous (and para-autochtonous) Mesozoic sedimentary

cover and the alochtonous Mesozoic sedimentary sequences in the nappe position. The degree of the Alpine metamorphic overprint and magmatic activity varies from low or negligible to substantial.

The Tatric part of the Nízke Tatry Mts. was an important historical source of Sb, Au, Fe, Cu, and other metals (Chovan et al. 1994, 2006). Stibnite ores were mined at the Dúbrava deposit until 1992 and Dúbrava was considered to be a moderate to large Sb deposit on the global scale. The nearby Magurka deposit was mined for Au and Sb until 1923 and used to belong to prominent gold deposits in Europe. Smaller Sb and Au reserves were mined intermittently at Dve Vody, Rišianka, Malé Železné, Husárka, Lom, and other deposits and occurrences. The most important ore mineral here was stibnite, accompanied by Pb–Sb sulfosalts, carbonates, and quartz. A number of siderite–sulfide veins, with a prominent concentration in the vicinity of Vyšná Boca (Ozdín & Chovan 1999) were mined for Fe, Cu, and Ag. The latter two metals were hosted by tetrahedrite, associated with quartz and a wide range of sulfosalts. The Soviansko deposit was mined for Pb (Luptáková 2007), with galena and sphalerite as the main sulfides, but the reserves are two small to merit further interest in this deposit. A detailed account of mineralogy of these and related deposits in the Tatric part of the Nízke Tatry Mts. is given in the companion paper (Majzlan et al. 2020).

Relative temporal relationships among the mineralisation stages (see Majzlan et al. 2020, and Table 1) is well established. The absolute temporal position of these stages is, however, a matter of long-standing debate, based on geological arguments and correlation with other crustal units. As an example, the ores of the large Dúbrava deposit were considered to be Variscan (Michalenko 1962; Ilavský & Sattran 1976), Alpine (Chovan 1981), or both Variscan and Alpine (Harman 1956; Jakeš 1963; Grecula 1971; Chovan et al. 2006). Given that these ore bodies are an integral, albeit small constituent of the Tatric Superunit, the lack of precise geochronological data is a problem that precluded their assignment to specific events in the tectonothermal evolution of this unit. On the other hand, the understanding of this evolution could certainly benefit from the temporal position of the hydrothermal ores because they are witnesses of significant fluid circulation and mineral deposition events.

Table 1: Stages of hydrothermal mineralisations in the Tatric Superunit (after Majzlan et al. 2020), arranged according to their relative age.

molybdenite
scheelite
arsenopyrite–pyrite–gold
stibnite–sphalerite–Pb–Sb-sulfosalts
dolomite–baryte–tetrahedrite
siderite–ankerite
quartz–tourmaline
quartz–Cu-sulfide
galena–sphalerite
baryte
hematite

In this work, we therefore focus on the ore deposits in the Nízke Tatry Mts. (NTM), a typical core mountain range of the Tatric Superunit, with a Variscan crystalline core and Alpine cover. Geochronogical data from ore mineralisations, presented only in open file reports or conference abstracts, are also included in the discussion. They pertain to ores in the Nízke Tatry Mts., Tatry Mts., Malé Karpaty Mts., and to parts of the Veporic Superunit directly adjacent to the Tatric part of the Nízke Tatry Mts.

A central tool which improved the ability to date ore mineralisations is the U/Pb LA–SF–ICP–MS analysis of hydrothermal carbonates. This method was extensively applied and it yielded ages relevant directly to the minerals which are related to the precipitation of sulfides. These data are augmented by U–total Pb dating and U/Pb/Th CHIME dating of uraninite and monazite, Re/Os molybdenite age determinations and Ar/Ar dating of illite. Additional, so far unpublished K/Ar and Re/Os ages are included in the discussion and placed in the context of the tectonothermal evolution of the CWC.

Geological setting

Alike the Pyrenees, Alps and/or Himalayas, the Carpathian mountain chain is a typical Alpine collisional fold belt. The Western Carpathians form a direct continuation of the Eastern Alps. The pre-Alpine crystalline basement crops out mainly in the CWC – the heart of the Western Carpathians, consisting of three principal crustal-scale superunits: the Tatric, Veporic and Gemeric and several cover-nappe systems like the Fatric, Hronic, Silicic and Meliatic (generally from N to S), see Plašienka (2018 and citations therein). The Variscan granitic rocks occur in all three superunits of the CWC in various positions. In the Tatric Superunit, granitic rocks form backbones of the so-called core mountains (Fig. 1). The core mountains of the Tatric Superunit are composed of pre-Mesozoic metamorphic rocks and granitoids, both overlain by Mesozoic cover sediments and nappe structures. Generally, felsic granitic magmatism dominated the Variscan orogeny over the time interval of 100 million years (365–250 Ma) in Europe. The CWC include different genetic types of granitic rocks, such as I-, hybrid I/S-, S-, A-, and specialised ore-bearing S_s-type, due to varying geotectonic settings (from subduction through crustal thickening and collision to orogenic collapse and extension) (Petrík & Kohút 1997; Kohút 2014 and citations therein; Broska & Kubiš 2018).

There are many similarities between the pre-Mesozoic basements of the stable Western Europe (e.g., the Massif Central or the Bohemian Massif) and the Variscan basement fragments within the Alpine–Carpathian orogenic belt. During the Alpine tectonism, this unstable part of the Variscan belt was disrupted, sliced into blocks, and incorporated into the Alpine (nappe and/or terrane) complexes, subsequently buried and finally uplifted. This polyorogenic history makes the reconstruction

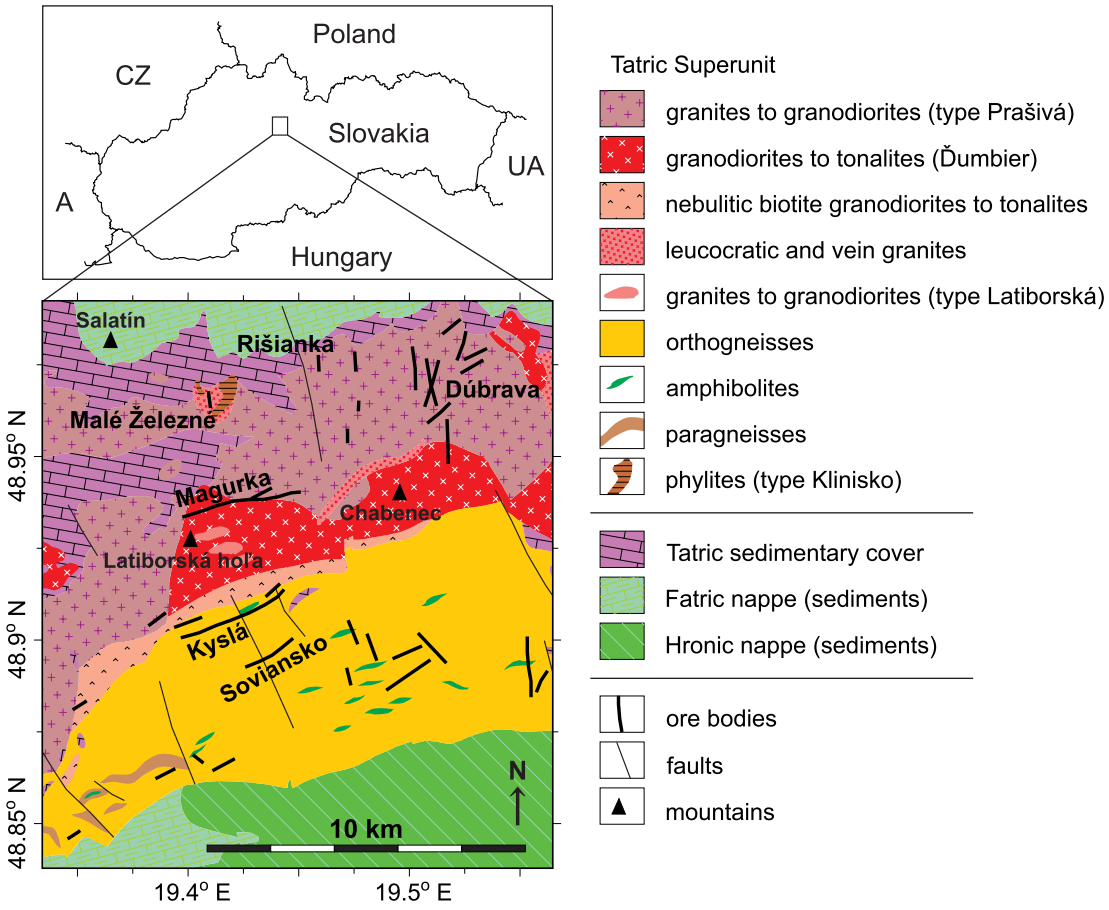

Fig. 1. Geological map of the central part of the Nízke Tatry Mts. with the deposits and occurrences mentioned in this work. Geological units and faults redrawn and simplified from Biely et al. (1992). Position of the veins taken from Chovan et al. (1996) and Bakos et al. (2000). For a complete geological map of the Nízke Tatry Mts. with names of all deposits and occurrences, see fig. 2a in Majzlan et al. (2020, this issue).

of the Variscan structures rather difficult, but provides an excellent exposure of various levels of the Variscan crust in the CWC.

The Nízke Tatry Mountains are situated in the northern sector of the central Slovakia and represent a typical multicomplex and polyorogenic part of the CWC. Geographically they form a 90 km long and 25 km wide E–W trending mountain range that is divided in the western (Ďumbier, Fig. 1) part belonging to the Tatric Superunit, and the eastern (Kráľova Hoľa) part which is formed by the Veporic Superunit. Various types of the Variscan granitic rocks were identified within the Ďumbier part of the NTM basement, e.g., medium-grained biotite tonalites to granodiorites (Ďumbier type), coarse-grained porphyritic biotite granodiorites to granites (Prašivá type) and muscovite–biotite leucogranites (Koutek 1931; Lukáčik 1981; Kohút 1998). These magmatic rocks occur together with other crystalline basement rocks such as orthogneisses, paragneisses, migmatites and amphibolites. The autochtonous to para-autochtonous Mesozoic sedimentary cover rocks (the so-called Tatric Envelope Unit) overlie these magmatic and metamorphic rocks. Two allochthonous Mesozoic units – the Fatric Unit (Križná nappe) and the Hronic Unit (Choč nappe) occur in a tectonically higher position. The crystalline basement together with its Mesozoic cover and these nappe complexes were juxtaposed through north-directed thrusting during the Upper Cretaceous. The Ďumbier part of the NTM forms a typical horst structure and was finally exhumed during the Alpine orogeny in the Eocene period (Danišík et al. 2011).

Hydrothermal ore mineralisations of the Tatric Superunit

Ore mineralisations in the Tatric Superunit were reviewed and extensively documented by Chovan et al. (1994, 1996, 1998) and Majzlan et al. (2020). The latter authors summarised the results of many studies, including those presented in the open file report by Chovan et al. (2006), and suggested that these ore mineralisations can be divided in the stages listed in Table 1.

A mineralisation stage (hereafter, a stage) is understood here as a single step in the process of formation of hydrothermal ores. The stages are separated from each other by

inter-mineralisation tectonics, seen by cross-cutting relationships, brecciated textures, etc. The mineral and chemical content of a stage is similar among different deposits and occurrences. Hence, it should be possible to assign a geological age to each of these stages.

The stages in Table 1 are arranged from the presumably oldest to the presumably youngest one. None of the deposits includes all stages but some of them, especially the larger ones, contain multiple stages. These deposits provided the opportunity to discern the relative timing of the stages.

The mineral content, alteration styles, fluid types, and stable isotope signatures of all these stages were discussed by Majzlan et al. (2020), based on published and unpublished data from many deposits and occurrences in the Tatric Superunit.

Materials

Samples for this study came from the deposits and occurrences in the Tatric Superunit of the Nízke Tatry Mts. The precise localisation and brief description of each sample is given in Supplementary Table S1. Macrophotographs of most of the samples are in Suppl. Figs. S1–S12.

Dúbrava: Most of the samples came from this large Sb–Au deposit, mined until 1992 for stibnite. During the period of mining, the deposit was investigated and an archive of well documented samples, collected by one of the co-authors (M. Chovan) served as the basis for this study. This multistage deposit consists of N–S striking veins and stockworks, hosted by the Variscan granodiorites and migmatites. It contains mineralisations that can be assigned to the scheelite, molybdenite, pyrite–arsenopyrite–gold, stibnite–sphalerite–Pb–Sb-sulfosalts, and dolomite–baryte–tetrahedrite stages (Chovan et al. 1995a; Michálek & Chovan 1998). Two alteration events, with higher and lower temperatures of formation, were recognised here (Orvošová et al. 1998).

Magurka: This deposit was mined until 1923, mostly for gold and to a lesser extent for stibnite. In terms of mineralogy, it is similar to the Dúbrava deposit, and contains the same mineralisation stages. Modern mineralogical research (Chovan et al. 1995b) has been done only on samples from the dumps. A significant difference is the orientation of the veins whose meaning is not yet understood. At Magurka, the ore veins strike is E–W.

Rišianka: This small occurrence is located westward of Dúbrava (Fig. 1). The N–S veins are mineralogically similar to those at the larger Dúbrava deposit (Majzlan et al. 1998). There is a number of other small occurrences with comparable mineralogy in the area between and near the Dúbrava and Magurka deposits (Fig. 1) – Malé Želené, Kľačianka, Oružné, and Krámec (Bakos et al. 2000; Hovorič 2008).

Soviansko: This Pb–Zn deposit near the village of Jasenie was exploited mostly on a small scale in Medieval times and explored in the 1960s. The deposit consists of one large and many subsidiary vein structures, located in biotite and two-mica gneisses. Mineralogy of the deposit was investigated during the exploration period by Pouba & Vejnar (1955); fluid inclusions, stable isotopes and thoughts about the origin of the deposit were presented by Luptáková (2007).

Malé Železné: This small Sb deposit near the village of Partizánska Ľupča was known since 18th century and explored in the 1950s (Michalenko 1959). Ore mineralisation consists of stibnite, various Pb–Sb sulfosalts, and quartz located in granitic or metamorphic rocks (Majzlan et al. 1998). Early quartz veins, pegmatites or silicified zones contain accessory molybdenite.

Methods

All samples were prepared in the form of polished and thin sections and examined in transmitted and reflected polarised light. Selected sections and minerals were further examined by an electron microprobe JEOL JXA-8230 (Jena) to obtain back-scattered electron (BSE) images, energy-dispersive (EDX) and wavelength-dispersive (WDX) analyses. For the hydrothermal carbonates the operating conditions were set to an accelerating voltage of 15 kV, a beam current of 15 nA and a beam diameter of 1–3 μm. Wavelength dispersive X-ray spectrometers were used to measure the elements and X-ray lines of Mg (Kα), Si (Kα), Sr (Lα), Ba (Mα), Ca (Kα), Mn (Kα) and Fe (Kα) with counting times of 40 s. The standard specimens used for calibration were: MgO for Mg, wollastonite for Si, celestine for Sr, baryte for Ba, apatite for Ca, rhodonite for Mn and hematite for Fe. The detection limits, calculated from the peak and background counts, the measurement time, the beam current and the standard material concentration were: 0.06 wt. % for Mg, 0.03 wt. % for Si, 0.09 wt. % for Sr, 0.09 wt. % for Ba, 0.02 wt. % for Ca, 0.05 wt. % for Mn and 0.05 wt. % for Fe.

Products of hydrothermal alteration of host rocks at the Jasenie-Soviansko deposit were characterised by means of powder X-ray diffraction (XRD) analysis of <2 μm grain size fractions. They were obtained by sedimentation method in distilled water in Attenberg cylinders. Before separation, samples were chemically treated to remove carbonates and Fe–Mn oxyhydroxides using standard procedure of Jackson (1975). Samples were analyzed in Ca-form both as oriented and random preparations. The XRD analyses were performed on Philips PW1710 diffractometer under following conditions: CuKα, 40 kV, 20 mA, secondary graphite monochromator, step: 0.02 °2θ, time per step: 0.8 or 1.25 s. Illite polytypes were identified according to criteria of Moore & Reynolds (1997). Quantitative compositions of illite polytypes were estimated with the method of Grathoff & Moore (1996).

Radiometric dating

Laser ablation–sector field–inductively coupled plasma–mass spectrometry (LA–SF–ICP–MS) was used for the *in situ* U/Pb isotopic analyses and dating in polished thick section at

the Goethe University Frankfurt (GUF). This method was used to date hydrothermal carbonates and quartz. At GUF, a ThermoScientific Element 2 sector field ICP–MS is coupled to a RESOLution S-155 (Resonetics) 193 nm ArF Excimer laser (CompexPro 102, Coherent) equipped with a two-volume ablation cell (Laurin Technic, Australia). Static ablation in a helium atmosphere (0.3 l/min) used a spot size of 213 µm and a fluence of ca. 1 J cm^{-2} at 6 Hz. Soda-lime glass SRM-NIST614 was used as a reference glass together with 3 carbonate standards to bracket sample analysis. Raw data were corrected offline using a macro-based in-house MS Excel© spreadsheet program (Gerdes & Zeh 2009). The $^{207}Pb/^{206}Pb$ ratio was corrected for mass bias (0.6 %/amu) and the $^{206}Pb/^{238}U$ ratio for inter-element fraction (ca. 5 %). Due to the carbonate matrix an additional correction of 9 % has been applied on the $^{206}Pb/^{238}U$, which was determined using WC-1 carbonate reference material dated by TIMS (254±6 Ma, Roberts et al. 2017). It was not possible to obtain reasonable data for every sample because of the low U content or unfavourable U/Pb ratio. About half of the carbonate samples used in this study yielded ages; for the other half, no data could have been obtained. The uranium and lead concentrations for the spots, which defined the isochrons and ages presented in this work, are shown in Suppl. Fig. S13.

Re/Os molybdenite methodology basically followed the procedures described in detail in Ackerman et al. (2017) utilizing the ^{185}Re spike–Os normal method (Selby & Creaser 2001). In brief, this includes decomposition of the samples in Carius Tubes using reverse aqua regia, Os separation by solvent extraction and Re separation by NaOH/acetone followed by ion exchange chromatography using AG 1×8 resin (Eichrom). Both rhenium and osmium fractions were subsequently analysed by negative thermal ionisation mass spectrometry (N-TIMS) on flattened Ni and Pt wires, respectively, using Thermo Triton Plus housed at the Czech Geological Survey (Prague). During the course of the study, several analyses of 1 ng Re solution (NIST 3134) yield $^{185}Re/^{187}Re$ value of 0.5976±11 (n=5) whereas 12 ng Os solution (UMCP Johnson-Matthey) yield $^{187}Os/^{188}Os$ of 0.11382±7 (n=10). All gathered data were corrected for the blank (8 pg for Re, 1.7 pg for Os) and total uncertainities of calculated model ages include Re decay constant uncertainty. The accuracy of the protocol was monitored through the analyses of NIST 8599 Henderson Mine molybdenite yielding the value of 27.73±0.23 Ma and 27.66±0.18 Ma, both values in excellent agreement with that of Markey et al. (2007).

Chemical Th/U/total Pb isochron method (CHIME) was applied to larger uraninite and monazite grains, using a Cameca SX-100 electron microprobe at the Dionýz Štúr State Institute of Geology (Geological Survey) in Bratislava. Analyses were carried out with 180 nA beam current, 15 kV accelerating voltage, and a beam diameter of 1 to 3 µm. Background levels were determined using a linear fit. The counting times (peak+ background) for Si, Al, Ca, P and As was 20 s, for REE 25 s, for Th and Y 35 s, for U 65 s and for Pb 150 s. The following standards were used: Si – wollastonite, Al – Al_2O_3, Ca – wollastonite, Pb – PbS, Th – ThO_2, U – UO_2, P – apatite, As – GaAs, S – pyrite, Fe – fayalite, Sr – $SrTiO_3$, REE and Y – REE and Y phosphates. Si, Al, As were measured with the use of a TAP crystal; Ca, Pb, U, Th, Y, P on LPET and REE on LLIF crystals. The following analytical lines were utilised: Kα for Si, Al, Ca, P, Fe, Sr and S, Lα for La, Ce, Gd, Tb, Tm, Yb, Y and As, and Lβ for Pr, Nd, Sm, Eu, Dy, Ho, Er and Lu. In order to determine concentrations of Pb and Th, Mα line was used, whereas determination of U was performed with Mβ spectral line. PAP corrections (Pouchou & Pichoir 1985) were applied throughout. All errors reported, depicted, and discussed in this paper are at the 2σ level (95 % confidence limits).

U–total Pb dating was applied also to minute uraninite grains with a Zeiss ULTRAPLUS field-emission scanning electron microscope (University Salzburg) equipped with back-scatter electron imaging capabilities and a large area silicon drift detector (Oxford X-MAX 50) (Waitzinger & Finger 2018). A synthetic Pb-free UO_2 crystal, crocoite ($PbCrO_4$) and Pb-containing glasses were used as calibration standards. An analytical precision of ≈0.3 and 0.16 wt.% (1σ) was achieved for U (Mα) and Pb (Mα) respectively, using a counting time of ≈1 minute per spot and an accelerating voltage of 15 kV. This analytical uncertainty corresponds to an age error of ≈16–17 Ma (1σ). Additional elements were measured in standardless mode (3σ detection limit 0.3–0.5 wt. %). Background, line interference and matrix corrections were made using INCA Energy software. Oxygen was generally calculated using the stoichiometry based on the cations (in case of uranium: UO_2) and not from the measured oxygen signal, as the latter is difficult to calibrate accurately and is oversensitive to surface contamination and oxidation. However, the oxygen (and carbon) peak intensities were routinely checked for anomalies in order to recognize any local alteration involving oxidation, hydration or carbonation. The accuracy of the dating procedure was monitored by measurements on an in-house uraninite reference material from Mitterberg, Austrian Greywacke Zone, which is dated at 91±5 Ma (Paar & Köppel 1978). Analysis of this standard shows good reproducibility with individual spot ages ranging between 80±17 and 103±17 Ma and a mean age of 93±6 Ma (n=14, MSWD=0.19).

Dating of illite/muscovite in altered hydrothermal rocks was performed by measuring the $^{40}Ar^*/^{39}Ar$ isotopic ratio at the Central European Ar-Laboratory – CEAL in Geological Institute of Slovak Academy of Science (Bratislava) equipped with VG 5400 Noble Gas Mass Spectrometer and special home-built Ar gas extraction line. Illite concentrates of 2–6 µm size fractions were loaded into glass tubes and irradiated together with sample monitors of known isotopic compositions in the nuclear reactor at the Nuclear Research Institute Řež (Prague). The irradiation J-values were determined with international standards including muscovite Bern 4M (Burghele 1987) and Fish Canyon sanidine (Renne et al. 1994; Jourdan & Renne 2007). Isotopic ages were calculated using decay constants reported by Steiger & Jäger (1977) and using the following correction factors for interfering isotopes:

$^{40}Ar/^{36}Ar_{air}$=299±1 %; $^{36}Ca/^{37}Ca$=0.00027; $^{39}Ca/^{37}Ca$=0.00039; $^{40}K/^{39}K$=0.0254. Argon was released using the stepwise heating technique (8 temperature steps from 590 to 1250 °C) using a resistance furnace and analysed on a VG-5400 Fisons noble-gas mass spectrometer following the analytical procedure of Frimmel & Frank (1998).

For the K/Ar dating of illite, 100 mg of illite powder was degassed in a conventional extraction device with induction heating. Isotopic composition of argon was measured via isotopic dilution in a mass spectrometer with a 90° magnetic sector type of 150 mm radius, operated in a static regime. Potassium was determined by flame photometry. All analytical uncertainties are represented at the 1σ level, corresponding to 68 % confidence level. The analytical techniques of K/Ar dating (ATOMKI, Debrecen, Hungary) were described in detail by Balogh et al. (1999). The K/Ar data presented in this paper were already published in an abstract of Chovan et al. (2010) with no specification of the details of the method.

Results

CHIME dating of uraninite from Dúbrava

Large (up to 1 cm) grains and crystals of uraninite occur in a granitic pegmatite body in Dúbrava. In our samples, the crystals are associated with large flakes of muscovite and crystals of K-feldspar, in agreement with the original description of the pegmatite (Dávidová 1998). Inspection of the back-scattered electron (BSE) images showed that the uraninite crystals are homogeneous, with abundant cracks but no signs of leaching or alteration (Fig. 2a). Spot chemical analyses (Table 2) also documented homogeneity of the crystals and revealed elevated concentration of U, Pb, Th, Y, and a number of rare earth elements. Each analytical datum served for the calculation of an apparent age and the final statistical evaluation gave the geological age of 343±1 Ma (Fig. 2b).

Re/Os dating of molybdenite

Two molybdenite samples from Dúbrava and Malé Železné yielded similar ages of 352±3 Ma and 351±3 Ma, respectively (Tables 3, 4). Their association with early quartz veins at Dúbrava or pegmatites at Malé Železné was indicative of their link with the high-temperature processes linked to the Variscan orogeny.

LA–SF–ICP–MS dating of quartz associated with illite and arsenopyrite

One of the samples studied, the sample 1, was found unsuitable for dating of the carbonate aggregates. Yet, the ablation of quartz, intermixed with illite and arsenopyrite crystals (Fig. 3), gave usable data and defined an isochron with an age of 320±8 Ma. In addition, another group of data points from this sample gave a younger age of 159±7 Ma.

LA–SF–ICP–MS dating of carbonates from the stibnite–sphalerite–Pb–Sb-sulfosalts stage

Samples from the Dúbrava (127, 112A, 52, 302, 131, VS-10), Magurka (K-13), and Rišianka (RIŠ-12) deposits were selected to represent this stage. Macroscopically, the samples show invariably close association of carbonates of the dolomite–ankerite series, quartz, and ore minerals – stibnite or Pb–Sb sulfosalts (most commonly zinkenite). The textures are interpreted as signs of coeval crystallisation of the carbonates and Sb minerals.

Inspection of BSE images showed that the carbonates are heterogeneous. There are three types of carbonates:

- massive dolomite–ankerite carbonates with essentially no other minerals (hereafter dol I carbonates)
- massive dolomite–ankerite carbonates intergrown with stibnite or Pb–Sb sulfosalts (hereafter dol II carbonates)
- siderite–magnesite carbonates (hereafter sid carbonates) that occur as relics in dol I carbonates, as disseminated minute

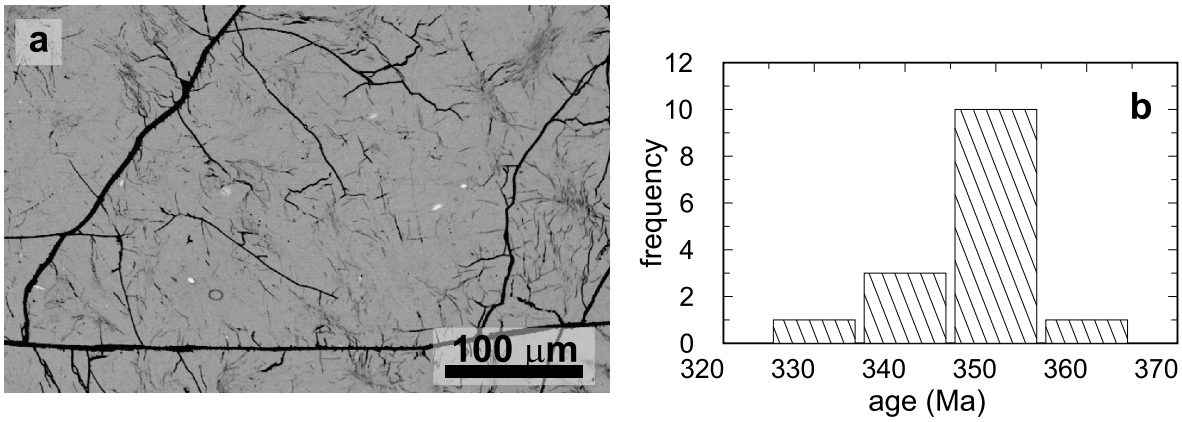

Fig. 2. a — BSE image of a homogeneous uraninite crystals from the pegmatite at Dúbrava; **b** — Age histogram for this uraninite.

Table 2: Representative EMP analyses of the uraninite crystals from pegmatite at the Dúbrava deposit.

Analysis no.	1	2	3	4
UO_2	91.01	90.57	90.74	90.38
SiO_2	0.03	0.04	0.04	0.04
As_2O_5	0.13	0.13	0.12	0.18
P_2O_5	0.02	0.01	0.01	0.01
PbO	4.19	4.28	4.16	4.24
ThO_2	0.89	0.87	0.87	0.97
Y_2O_3	0.46	0.48	0.41	0.43
SO_3	0.02	0.05	0.02	0.08
CaO	0.07	0.06	0.26	0.02
Ce_2O_3	0.13	0.12	0.03	0.05
Pr_2O_3	0.30	0.33	0.29	0.34
Sm_2O_3	0.20	0.25	0.17	0.18
Eu_2O_3	0.22	0.20	0.24	0.23
Gd_2O_3	0.32	0.30	0.30	0.31
Tb_2O_3	0.08	0.10	0.14	0.04
Dy_2O_3	0.10	0.17	0.15	0.14
Ho_2O_3	0.07	0.00	0.03	0.04
Er_2O_3	0.54	0.58	0.57	0.52
Tm_2O_3	0.08	0.08	0.11	0.14
Yb_2O_3	0.26	0.25	0.26	0.25
Lu_2O_3	0.18	0.14	0.09	0.16
Total	**99.29**	**99.01**	**99.01**	**98.77**

Table 3: Rhenium and osmium concentrations in the two dated molybdenite samples, with the calculated model ages.

Sample	Locality	Re (ppm)	2σ	^{187}Os (ppb)	2σ	Model age (Ma)	2σ
602	Dúbrava	30.67	0.07	113.3	0.7	351.8	2.6
MŽ-1	Malé Železné	40.58	0.09	149.4	0.9	350.5	2.5

grains in the altered rocks, or as larger aggregates in altered rocks, in the latter case intergrown with dolomite–ankerite carbonates, chlorite and illite.

Only the dol I and the sid carbonates were used for dating. All attempts to use the dol II carbonates failed because these carbonates contain too much lead. Both dol I and dol II carbonates are chemically variable but there is a subtle difference between the two groups. The dol I carbonates appear darker in the BSE images (Fig. 4a, b) and are Mg-richer than the dol II carbonates; the dol II carbonates are Fe-richer. The dol II carbonates appear to be younger and penetrate into the dol I carbonates in a form of thin veinlets, accompanied by small sulfide grains (Fig. 4a). In some cases, relics of the darker dol II carbonates are observed in the dol I carbonates (Fig. 4b).

The sid carbonates are fine-grained, inhomogeneous (Fig. 5a) and comprise members of the siderite–magnesite and dolomite–ankerite series. The siderite–magnesite grains contain patches of material richer in Fe and richer in Mg, as seen clearly in BSE images (Fig. 5a). All these carbonates are intergrown with quartz and alteration sheet silicates (chlorites, illite).

The geochronological results from the samples that yielded data are shown in Fig. 6 and Table 4. Some of the samples defined isochrones constrained with sufficient data points and resulting in excellent statistics (Fig. 7c). Some of the data sets carry signs of younger processes and two or even three ages can be extracted (Fig. 7a). In one case, for the sample RIŠ-12, the U content in the carbonate was sufficient for the purposes of dating but the data scatter was so large that any age between 300 and 25 Ma could have been chosen (Fig. 7b).

The older group of ages determined in the samples from Dúbrava extends from 342±49 to 325±9 Ma. The sample K-13 from the Magurka deposit gave a slightly different age of 286±37 Ma. In most samples, younger ages were also observed, corresponding either to the Jurassic/Cretaceous boundary, Upper Cretaceous, or Miocene (see Fig. 6 and below).

LA–SF–ICP–MS dating of carbonates from the dolomite–baryte–tetrahedrite stage

Samples from the Dúbrava deposit (131, 40, 54, 125, U 13) were selected for this work. They consist of dolomite, quartz, baryte, and tetrahedrite, occasionally associated with chalcostibite. Tetrahedrite from this stage is typical by its high Sb/(Sb+As) ratio (>0.9) and variable Zn/(Zn+Fe) ratio.

The BSE images document multiple stages of cracking, healing, and replacement (Fig. 8). Such complex internal texture is characteristic of all observed samples. In terms of their chemical composition, all carbonates of this stage belong to the dolomite–ankerite series (Fig. 9). They differ only by their Mg/(Fe+Mn) ratio.

Several samples gave an acceptable isochron or two distinct isochrons and the results are summarised in Fig. 6 and in Table 4. Most samples assigned to this stage gave ages between 159±7 and 128±4 Ma, corresponding to the Paleoalpine uppermost Jurassic and lowermost Cretaceous periods. Such ages were also detected in the samples 1 and 52 which gave also an older (Variscan) age, thus documenting carbonate remobilisation during the Paleoalpine period. Some of the samples returned Paleoalpine and younger ages, falling between 20 and 30 Ma.

Three samples (131, 125, U 13) gave only young ages of 31±2, 22±2, and 24±4 Ma, respectively. The sample 131, considered to be one of the best examples of tetrahedrite mineralisation at Dúbrava, contains mostly tetrahedrite hosted by quartz. Carbonates fill voids in quartz, sometimes lined by euhedral quartz crystals (Fig. 5b), and are clearly younger than the tetrahedrite and quartz.

Ar/Ar dating of illite from Jasenie-Sovіansko

Host rocks of this galena–sphalerite deposit are different types of para- and orthogneisses, with primary quartz, plagioclase, biotite, and less abundant muscovite and K-feldspar. Hydrothermal alteration has caused extensive appearance of secondary illite, carbonates, quartz, chlorite, and albite. The intensity of the alteration increases markedly

Table 4: Geochronological data for the ore mineralisations obtained and reviewed in this work. The ages of the host rocks are reviewed and summarised in the text. Precise localisation of the samples is listed in Table S1. Macrophotographs of many of these samples are in Figs. S1–S12.

Sample, mineral dated (locality)	Method	Age (Ma)	Notes
molybdenite (Dúbrava)	Re/Os	343±4	Chovan et al. (2010)
602, molybdenite (Dúbrava)	Re/Os	352±3	molybdenite in quartz veinlets
MŽ-1, molybdenite (Malé Železné)	Re/Os	351±3	molybdenite in quartz veins/pegmatites
814 and 828, monazite (Dúbrava)	U/Pb/Th CHIME	345±2	monazite in altered rocks, Chovan et al. (2006)
uraninite (Dúbrava)	U/Pb/Th CHIME	343±1	uraninite in pegmatite
biotite (Kyslá)	K/Ar	330±5	biotite in pegmatite, Molák et al. (1989)
biotite (Kyslá)	K/Ar	305±4	biotite related to scheelite mineralisation, Molák et al. (1989)
A-6a, illite (Dúbrava)	K/Ar	218±8	Chovan et al. (2006)
A-10, illite (Dúbrava)	K/Ar	117±5	Chovan et al. (2006)
A-11, illite (Dúbrava)	K/Ar	193±7	Chovan et al. (2006)
1-A, illite (Dúbrava)	K/Ar	201±8	Chovan et al. (2006)
NASH-19, illite (Pezinok)	K/Ar	179±7	Chovan et al. (2006)
NASH-20, illite (Pezinok)	K/Ar	172±7	Chovan et al. (2006)
1, quartz (Dúbrava)	U/Pb LA–SF–ICP–MS	320±8; 159±7	quartz associated with illite and arsenopyrite
112a, Fe-dolomite (Dúbrava)	U/Pb LA–SF–ICP–MS	334±12	Fe-dolomite associated with stibnite
52, Fe-dolomite (Dúbrava)	U/Pb LA–SF–ICP–MS	325±9; 128±4; 72±4	Fe-dolomite associated with quartz and stibnite
K-13, Fe-dolomite (Magurka)	U/Pb LA–SF–ICP–MS	286±37; 30±6	Fe-dolomite associated with stibnite
302A, Fe-dolomite (Dúbrava)	U/Pb LA–SF–ICP–MS	342±49, 17±2	Fe-dolomite associated with stibnite
VS10/4, Fe-dolomite (Dúbrava)	U/Pb LA–SF–ICP–MS	324±6	Fe-dolomite associated with stibnite
131, Fe-dolomite (Dúbrava)	U/Pb LA–SF–ICP–MS	31±1	Fe-dolomite in quartz with tetrahedrite
40, Fe-dolomite (Dúbrava)	U/Pb LA–SF–ICP–MS	135±13; 22±2	Fe-dolomite associated with tetrahedrite
54, Fe-dolomite (Dúbrava)	U/Pb LA–SF–ICP–MS	156±13; 23±1	Fe-dolomite associated with tetrahedrite and chalcostibite
125, Fe-dolomite (Dúbrava)	U/Pb LA–SF–ICP–MS	22±2	Fe-dolomite associated with chalcostibite
U 13, Fe-dolomite (Dúbrava)	U/Pb LA–SF–ICP–MS	24±4	Fe-dolomite with tetrahedrite veinlets
RIŠ-3, uraninite (Rišianka)	U/Pb CHIME	70±6	colloform uraninite

in the immediate vicinity of the ore veins. In the zone directly adjacent to the veins, the rocks are almost completely bleached, with relics of primary rock-forming minerals. Here, illite replaced all minerals except for quartz, and crystallised also in small vugs in the altered rocks.

The sample 6/98 (Fig. 10a), selected for a further detailed study, shows distinct variations in the properties of the alteration illite. The full width at half maximum (FWMH) of the 00l diffraction peaks is 0.28–0.32 °2θ, typical for illite with high crystallinity. The number of expanding interlayers is very small (<5.5 %), as judged from the Ir index of 1.20–1.35 (cf. Środoń & Elsass 1994). The b_0 parameters (9.036–9.035 Å), calculated from the positions of the 060 diffraction maxima, are typical for dioctahedral illite with increased Fe content. The fine-grained fraction (<2 μm) is a mixture of several polytypes, in order of abundance $2M_1>1M_d>1M_t$.

The subsample 6/98/3 was taken directly at the contact of the ore veins and altered rock. In this subsample, illite completely replaces all rock-forming minerals except for quartz. In addition, this subsample contains abundant carbonates, hematite, Ti-oxides, and pyrite. The subsample 6/98/1 was taken about 15 cm from the vein-rock contact. It contains large flakes of metamorphic muscovite, partially replaced by illite. Biotite and chlorite are missing completely; either these rocks never had such sheet silicates, or they were completely altered to illite. Feldspars were also mostly converted to illite, although feldspar relics can be recognised. The $2M_1$ polytype is the most abundant one throughout the profile but its abundance decreases with the distance from the vein, at the expense of the $1M_d$ polytype.

The two subsamples 6/98/1 and 6/98/3 were chosen for Ar/Ar dating. Both of them show consistent negative staircase pattern (Fig. 10) where the rims gave apparent older ages than the cores. The maximum crystallisation ages are 96 and 105 Ma, respectively. In addition, both samples show the last high-temperature step of distinctly higher age, related to argon release from a small portion of older micas.

U–total Pb dating of the uranium mineralisation from Rišianka

The uranium mineralisation at Rišianka consists of colloform pyrite, uraninite, coffinite, and galena, finely disseminated in a strongly silicified and altered rock (Fig. 11a). The silicification produced fine-grained quartz and/or chalcedony, locally associated with illite. The mineralisation was described by Daniel et al. (1984) who also reported cinnabar as one of the primary sulfides. Pyrite could be locally weathered to iron oxides. There are thin-tabular crystals of uranium minerals, described as uranophane and gummite by Daniel et al. (1984). These crystals which appear as weathering products of uraninite are, however, associated with unweathered pyrite and galena. Their secondary origin can be thus questioned.

The uraninite occurs in globular intergrowth with coffinite (Fig. 11b, c). The challenge was to find larger homogenous uraninite domains which allowed a phase-pure analysis. Twenty-nine spot analyses show that the uraninite is characterised by an UO_2 content of close to 90 wt. %. In addition, it contains 3–7 wt. % Sb_2O_3 and minor contents of As_2O_3 (up to 1 wt. %), CaO (0.4–0.7 wt. %) and SiO_2 (0.1–0.3 wt. %). Th and Y occur in traces but the contents are always below the 3σ detection limit (<0.4 wt. %). The analytical totals of most uraninite analyses are slightly lower than 100 wt. %. This may result from unquantified minor element contents (Th, Y, etc.) and a potential presence of UO_3.

Measured PbO contents are between 0.71 and 0.99 wt. % and correspond to total Pb ages between 57±17 and 82±16 Ma (Fig. 11d). The mean total Pb age of all analyses is 70±6 (*n*=29, MSWD=0.14) and is interpreted as the formation age of the uraninite.

The disseminated uranium ores are cut by veinlets of coarse-grained, clear quartz cut by fractures perpendicular to the vein walls. The veins also contain weathered carbonate of the dolomite–ankerite series (Fig. 11a) and Pb–Sb sulfosalts with atomic Pb/Sb ratio of 0.5, close to zinkenite or scainiite (Table S2).

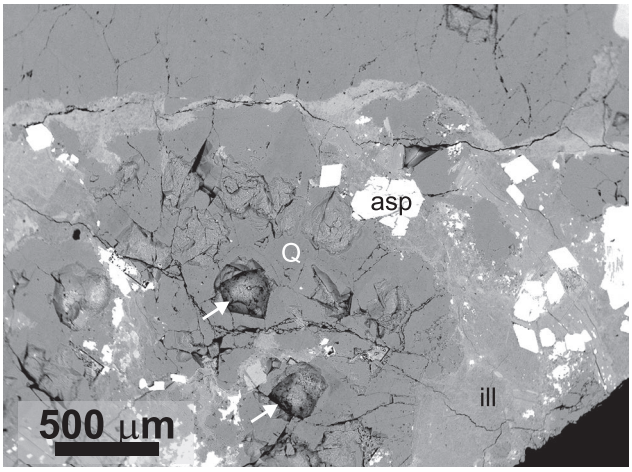

Fig. 3. BSE image of the sample 1, showing ablation spots (highlighted by arrows) in quartz (Q) associated with euhedral arsenopyrite (asp) and fine-grained illite (ill).

Discussion

Table 1 lists the mineralisation stages in their relative temporal relationships, determined from macro- and microtextures on many samples. Although the relative ages are well established, the "absolute" ages and hence the correlation of the mineralisations to the tectonothermal evolution of the Western Carpathians are largely missing. The Pb model ages of Chernyshev et al. (1984) are probably compromised by systematic errors and will not be further considered here. They indicate, for example, late Variscan ages for galena in a vein that penetrates into Triassic sediments at Trangoška, thus making the other data also doubtful.

Geochronology of the host rocks and ore mineralisation stages

Host rocks

The Dúbrava, Magurka, and Rišianka deposits, as well as a number of similar deposits in the NTM (Fig. 1), are hosted by Variscan granitic and high-grade metamorphic rocks. The K/Ar cooling ages on muscovite and biotite bracket the ages between 340 and 330 Ma and are also supported by Ar/Ar muscovite cooling age from the Klinisko granite with

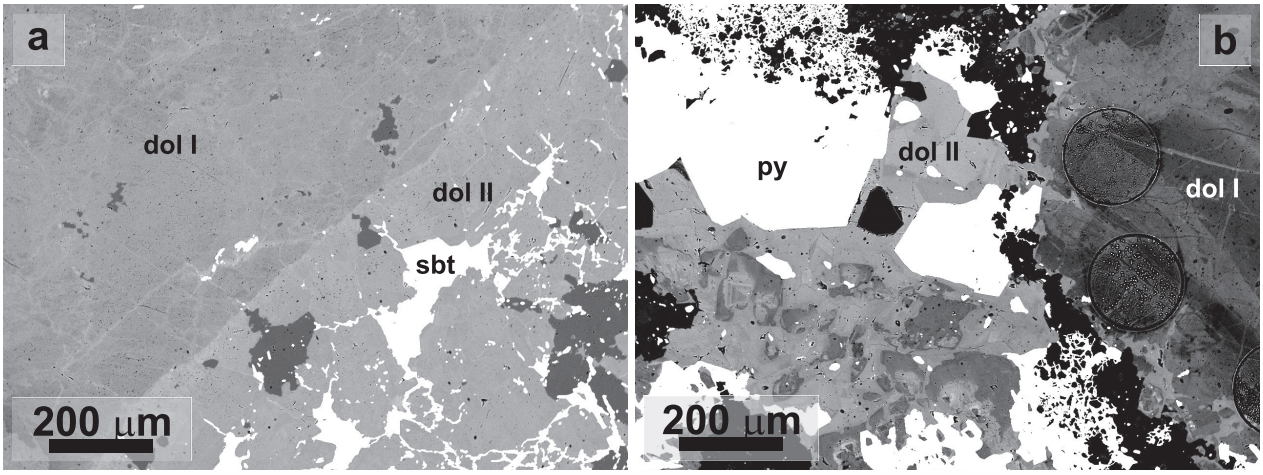

Fig. 4. BSE images of carbonates and sulfides that belong to the stibnite–sphalerite–Pb–Sb-sulfosalts stage. **a** — The contact between sulfide-poor dol I carbonate and younger sulfide-rich dol II carbonate. Sulfides are represented by stibnite (sbt). Sample K-13, Magurka. **b** — Darker, older dol I carbonate is being replaced by younger dol II carbonate. The dol I carbonate also forms relics in the dol II carbonate. The sulfide grains belong to pyrite (py). Note the large circular ablation spots in dol I. Sample 112A, Dúbrava.

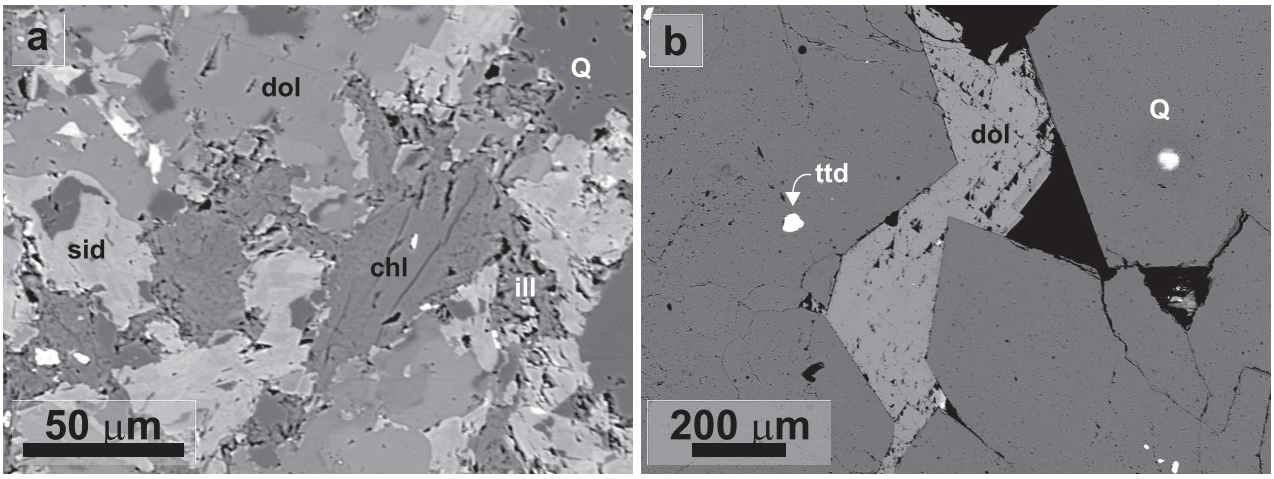

Fig. 5. a — BSE image of an alteration zone composed of sid carbonates – an intergrowth of siderite-magnesite carbonates (marked sid in the image), dolomite-ankerite carbonates (dol), chlorite (chl), illite (ill) and quartz (Q). Note that the siderite-richer compositions (marked in the image) contain also darker inclusions of magnesite-richer carbonates. Sample VS10-4, Dúbrava. **b** — Quartz (Q) with inclusions of tetrahedrite (ttd) hosts young dolomite–ankerite carbonates (dol) in the vugs. Sample 131, Dúbrava.

an age of 340±2 Ma (Kráľ & Štarková 1995). Whole-rock Rb/Sr results (Bagdasaryan et al. 1985) provided 362±21 Ma as the common isochrone age for the Ďumbier and Prašivá granite types and 365±17 Ma for the Králičká leucogranite. It is assumed that the Upper Devonian/Lower Carboniferous age of the Ďumbier and Prašivá granites in the Rb/Sr isotopic system represents the primary melting event of the lower crustal sources during the subduction processes, and can be considered as the possible oldest age of the Variscan NTM granitic rocks. Multigrain zircon dating of the Ďumbier granodiorite–tonalite brought an age of 343±3 Ma (Putiš et al. 2003). On the other hand, the cathodoluminescence-controlled single zircon U/Th/Pb dating results of the Ďumbier granodiorite from the Chopok area provided somewhat younger age of 330±10 Ma (Poller et al. 2001). Finally, single-grain dating on zircon yielded 356±2 Ma for the Ďumbier biotite tonalite and 353±3 Ma the Prašivá biotite granodiorite (Broska et al. 2013). Dioritic rocks from the Bor locality have a concordia age 350±2 Ma (Uher et al. 2011), while the youngest zircons from the Ďumbier biotite tonalite form a concordia with an age of 340±3 Ma (Kohút, unpublished data). Recent single-grain LA–ICP–MS zircon and apatite dating of diorite from Železné provided consistent results with 362±3 Ma for zircon concordia age and 358±3 for apatite (Spišiak, personal communication). In summary, the Variscan granitic rocks in the NTM form a composite massif which was formed during two principal phases of the Variscan orogeny. Basic I-type and hybrid I/S-type granitic rocks (e.g., diorites, tonalites, granodiorites) were produced during the subduction at 362–353 Ma from the recycled lower crustal sources in the volcanic arc environment. Later, during a maximum of the continental stacking and peak of continental collision period (340–330 Ma), mainly felsic anatectic magmas were generated in the middle or perhaps lower crust. This event affected the pre-existing granitic bodies by thermal overheating to extensive partial anatexis caused by the collapse of the orogen and/or rapid exhumation due to extension in compression. Different types of magmas were not homogenised because of the lack of time. The result is the NTM composite granitic body with two varieties of boundaries between the principal granite types (Ďumbier, Prašivá), i.e. mutual transitional and/or sharp contrasting borders.

Banded and augen orthogneisses are common constituents of the NTM crystalline basement. In the past, they were referred to as stromatitic or ophtalmitic migmatites and their importance was often overlooked (see review by Kohút 2004). Their protolith was dated by single-grain zircon U/Th/Pb method to 485–470 Ma (Putiš et al. 2009). Other radiometric results (U/Th/Pb, Rb/Sr isochrone, Ar/Ar, K/Ar) for the NTM orthogneisses are more or less compatible with shear deformation and metamorphism before 365 Ma, partial anatexis (335 Ma), and final rapid cooling at 332±2 Ma (Dallmeyer et al. 1996). A frequent member of the metamorphic pile in the NTM are banded amphibolites that are seen as analogues of the leptyno-amphibolite complex in Western Europe. SHRIMP zircon dating gave 481±4 Ma for a mafic – amphibolite layer and 480±5 Ma for a pale trondhjemite band (Putiš et al. 2009), suggesting that these rocks represent a mafic counterpart to the felsic orthogneisses. However, it is not clear if the scarce Ar/Ar amphibole ages of 410–395 Ma and 368–364 Ma reflect an ultrahigh-pressure metamorphic event or just limited opening of the Ar system due to the Variscan subduction metamorphism (Kantor & Eliáš 1983; Maluski et al. 1993; Dallmeyer et al. 1996).

Our work supports the above-mentioned data in general. The uraninite crystals from a granitic pegmatite at the Dúbrava deposit gave an age of 343±1 Ma, very similar to the 343±3 Ma, 344±3 Ma, 340±3 Ma and 330±10 Ma reported for the host tonalite–granodiorite (see above).

Chemical (CHIME) dating of monazite from the Dúbrava deposit gave 345±2 Ma (Chovan et al. 2013). Very similar age

of 341±15 Ma was determined on monazite from the Martina adit (Kriváň, Tatry Mts), associated with thorite, zircon, allanite, and rutile in mylonite zones in granitoid rocks (Chovan et al. 2006). Essentially identical CHIME monazite ages between 339±7 and 332±5 Ma have been presented from granites in nearly all Variscan Tatric Superunit core mountains (Kohút 2017), showing that this monazite and the associated minerals are rock-forming minerals, with no link to hydrothermal events.

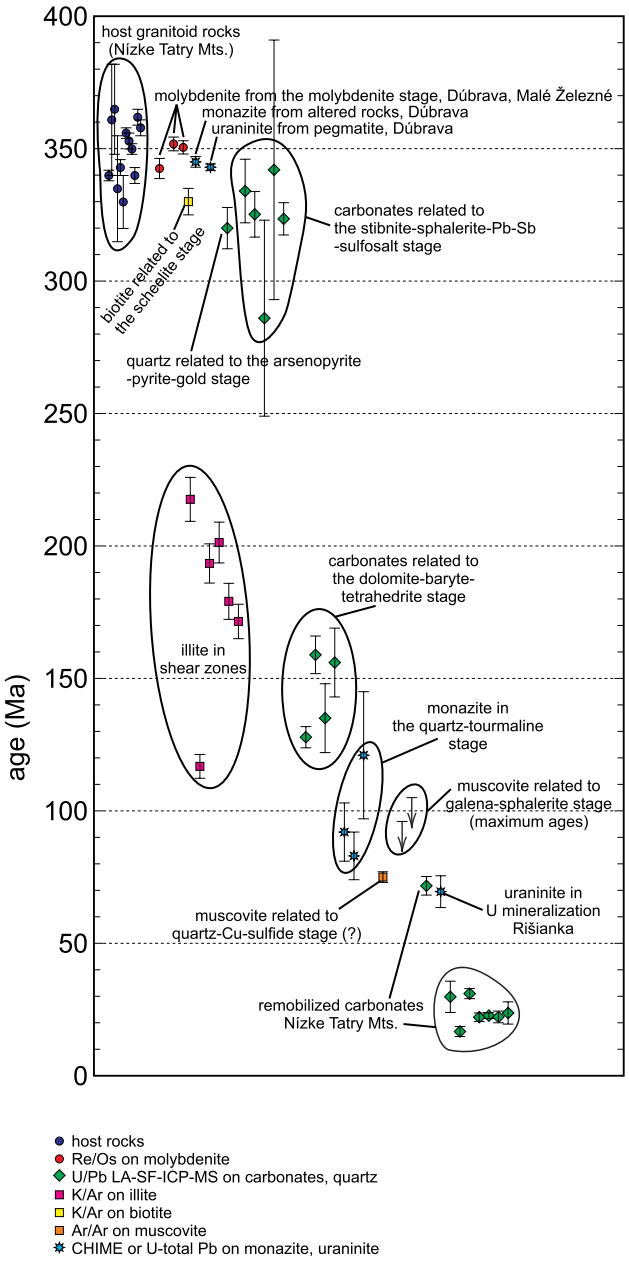

Fig. 6. Graphical summary of the data obtained and reviewed in this work, together with the age data for the host rocks of the mineralisations considered here. Numerical values and references are given in Table 4 and in the text. For clarity, the data may be offset horizontally.

Molybdenite and scheelite stages

Molybdenite from the Dúbrava deposit was dated by Re/Os method to 343±4 Ma (Chovan et al. 2013) and 352±3 Ma (this work), in a good agreement with the U/Pb zircon age of the host tonalite–granodiorite in the Nízke Tatry Mts (e.g., 353±3, Broska et al. 2013). Molybdenite was also reported by Michalenko (1959, 1960) and Majzlan et al. (1998) in muscovite pegmatites and quartz veins at the Malé Železné deposit. Its Re/Os age of 351±3 Ma (this work) also documents its genetic association with the host rocks. Rare molybdenite from the Západné Tatry Mts pegmatite in the granitic rocks was dated to 350±1 Ma (Mikulski et al. 2011).

Scheelite mineralisation, with a prominent deposit in Kyslá (Bláha & Bartoň 1991) and a subordinate occurrence in Dúbrava, was dated indirectly by K/Ar measurements on sheet silicates. A pegmatitic vein at Kyslá was dated to 330±5 Ma on biotite (K/Ar closure temperature of 300 °C) (Molák et al. 1989) but it is not clear how pertinent is this datum to the scheelite itself.

The host rocks of the Kyslá scheelite deposit were formed within the Lower Paleozoic (Cambrian–Ordovician) volcano-sedimentary formation of a back-arc basin (BAB) origin. The entire volcano-sedimentary sequence was subducted and metamorphosed during BAB amalgamation, producing amphibolites (perhaps also eclogites) from gabbros and leucocratic orthogneisses (perhaps also granulites) from granites. This sequence resembles to a great extent the leptyno-amphibolite complex (LAC) of the Western Europe, particularly at the Felbertal (Mittersill) scheelite deposit in the Eastern Alps. It is the type locality for stratabound scheelite deposits and is also hosted by a Cambro–Ordovician metavolcanic arc sequence with minor Variscan granitoids (Eichhorn et al. 1995; Raith & Stein 2006). If this analogy holds, then the earlier mineralisation at the Kyslá deposit was connected to the origin of the Lower Paleozoic volcano-sedimentary formation, whereas the Variscan mineralisation was related to the two principal phases of orogenic evolution. The first phase was the subduction, shear metamorphism and the first intrusion of the arc granites (362–353 Ma). The second phase comprised an important remobilisation of ore fluids that was induced by the anatexis and intrusion of collisional Variscan granites (340–330 Ma) during the peak of the crustal thickening.

Arsenopyrite–pyrite–gold stage

The age of the arsenopyrite–pyrite–gold mineralisation is not well constrained although this mineralisation used to belong to the economically most important ones. In this work, only sample 1 (Dúbrava) could be tentatively assigned to this mineralisation. Ablation of quartz associated with arsenopyrite (Fig. 3) gave the age of 320±8 Ma.

The geological position of the arsenopyrite–pyrite–gold mineralisation and its low-salinity, CO_2-rich fluids hint at its affinity to orogenic gold deposits (e.g., Goldfarb & Groves 2015), hence supporting rather its Variscan age. The Alpine

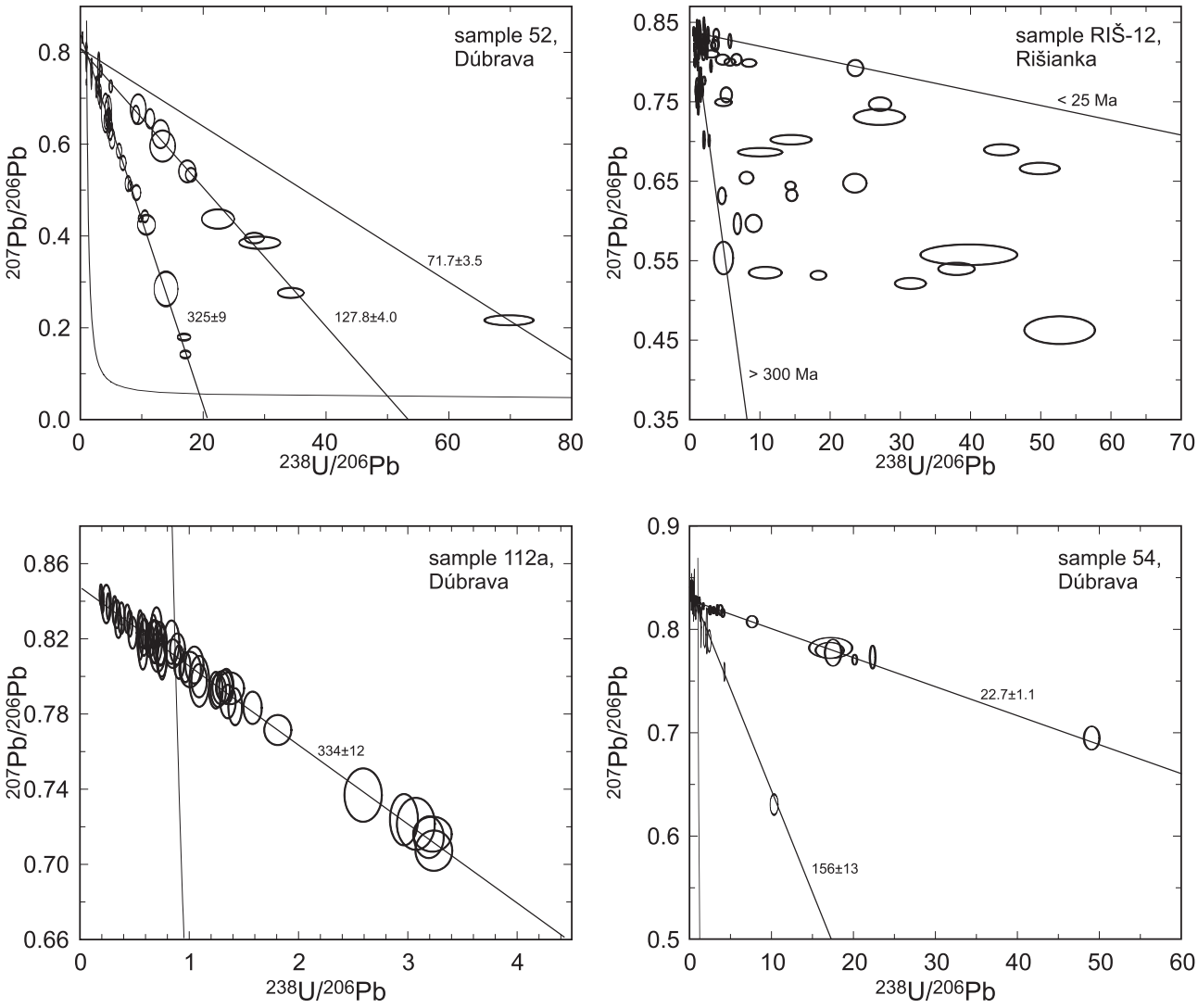

Fig. 7. Tera-Wasseburg diagrams for selected samples dated by U/Pb LA–SF–ICP–MS.

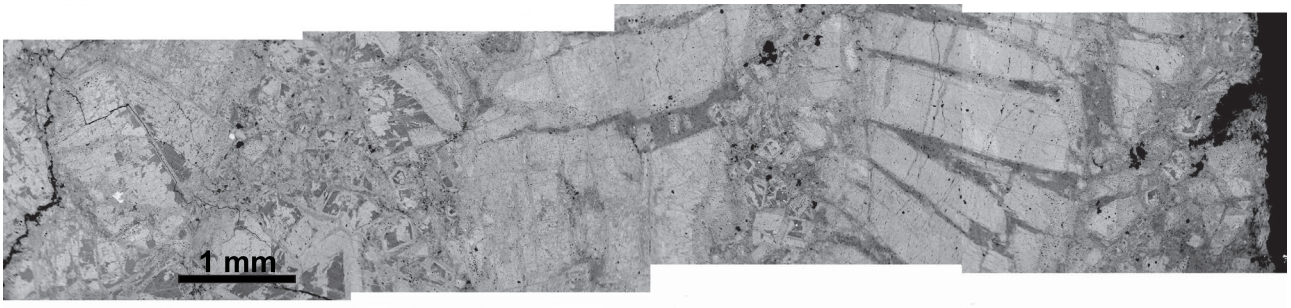

Fig. 8. Composite back-scattered electron image of the carbonates in the sample 40 from Dúbrava. They all belong to the dolomite–ankerite series, with variable Mg/(Fe+Mg) ratios. These ratios cause also the variations in the shades of grey visible in the image.

metamorphic overprint of the Tatric Superunit (Plašienka et al. 1997) may have been insufficient to generate such mineralisations, even though Danišík et al. (2008, 2010) and Anczkiewicz et al. (2015) demonstrated low grade metamorphism of the crystalline basement at temperatures >240 °C due to tectonic burial during the Eo-Alpine collision in the Late Cretaceous. Bakos et al. (2004) used geological arguments to underpin the Variscan age of gold–quartz veins in Harmanec.

These veins are hosted by orthogneisses in Starohorské Vrchy Mts., considered to belong to the Veporic Superunit (Polák et al. 2003) or to a transitional zone between the Tatric and Veporic Superunits (Plašienka 2003).

Textural evidence speaks undoubtedly for the older age of the pyrite–arsenopyrite–gold stage than the stibnite–sphalerite–Pb–Sb-sulfosalts stage (Majzlan et al. 2020). In this work, the stibnite–sphalerite–Pb–Sb-sulfosalts stage was found to be of Variscan age (see below), thus confirming also the Variscan age of the pyrite–arsenopyrite–gold stage.

Stibnite–sphalerite–Pb–Sb-sulfosalts stage

There are no previously published geochronological constraints for the stibnite–sphalerite–Pb–Sb-sulfosalts stage, despite its economic importance in the past and economic prospects in the future.

As described above, the samples from this stage contain three different types of carbonates: dol I, dol II, and sid carbonates. On a hand specimen or outcrop scale, there is no indication of several distinct carbonate generations, such as cross-cutting veinlets or brecciated textures. The dol II carbonates are clearly younger but they replace the dol I carbonates only as thin veinlets along the grain boundaries and small cracks. A smooth contact between the dol I and dol II carbonates (Fig. 4) suggest overgrowth of the older dol I by the younger dol II rather than metasomatic replacement or deposition in open fissures of the older carbonates. We interpret the observations made (Fig. 4) as an initial precipitation of a slightly Mg-richer dol I carbonate (without sulfides), followed shortly thereafter by feeding of metallic elements into the hydrothermal systems, including Sb, Pb, but also Fe. The increased concentration of these metals and their precipitation caused formation of stibnite or sulfosalts and the shift of the chemistry of the carbonates toward Fe-richer dol II compositions. The sid carbonates can be interpreted as the earliest carbonate precipitates related to incipient breakdown of biotite during the high-temperature alteration event.

We were able to attach dates only to the dol I and sid carbonates (see above). The ablation spots in dol I included sometimes thin veinlets of dol II. The ablation spots in the sid carbonates contain a mixture of siderite–magnesite and dolomite–ankerite carbonates, plus alteration chlorite or illite; textural evidence suggests that all these minerals formed simultaneously. Even though different carbonates were abladed in many of the selected spots, the samples still define one or two isochrons. This observation, together with the interpretation that the temporal differences between the various carbonates are small, leads to a conclusion that the dating results obtained from the dol I and sid carbonates can be applied also to the dol II carbonates and, therefore, also to the sulfides.

The six isochrons from these samples defined ages (Table 4) that average to 322 Ma, comparable to the 320 Ma tentatively assigned to the arsenopyrite–pyrite–gold stage.

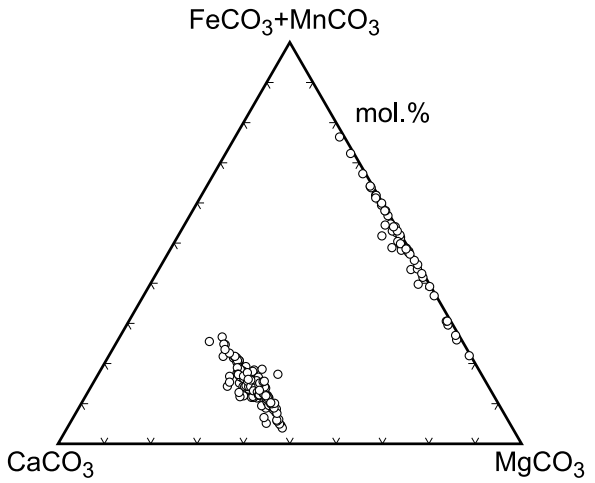

Fig. 9. Chemical composition of the hydrothermal carbonates from Dúbrava in the samples used for dating.

Dolomite–baryte–tetrahedrite stage

The U/Pb dating of the dolomite–ankerite associated with quartz and tetrahedrite gave two groups of ages. One of them spans from 159±7 to 128±4 Ma, averaging around 144 Ma, in the lowermost Cretaceous. The second group is much younger, of Miocene age (Table 4). Based on these measurements, the dolomite–baryte–tetrahedrite stage is assigned Upper Jurassic–Lower Cretaceous age. The younger ages relate to

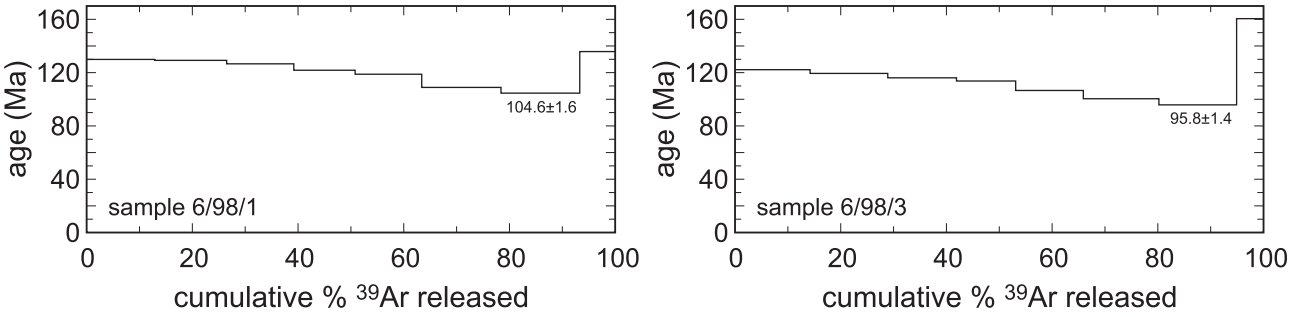

Fig. 10. $^{40}Ar/^{39}Ar$ apparent age spectra of the samples 6/98/1 and 6/98/3, Soviansko.

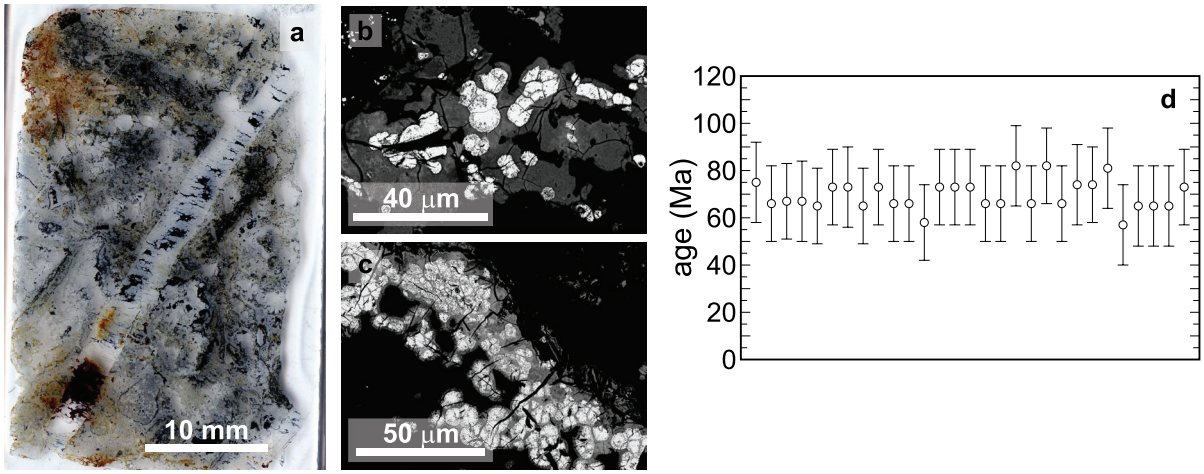

Fig. 11. a — An overview of the thin section RIŠ-3, Rišianka. Most of the section is built by a strongly silicified mass with dispersed uranium mineralisation that is cut by a quartz veinlet with dolomite (lower left corner) and aggregates of sulfosalts. **b, c** — BSE images of the uranium mineralisation, showing globular uraninite aggregates (white) surrounding by coffinite (grey) and quartz (black). **d** — CHIME ages determined for all spot analyses in the section RIŠ-3. They give the age of 70±6 Ma for uraninite.

the products of remobilisation, present in every sample (Fig. 8). Textural evidence, especially in the sample 131 (Fig. 5b), documents clearly that the Miocene carbonates postdate the tetrahedrite mineralisation.

Siderite–ankerite, quartz–tourmaline, and quartz–Cu-sulfide stages

There are only meager geochronological data for the siderite–quartz–sulfide veins so far. Pršek & Chovan (2001) reported that such veins by Bacúch (in the Veporic Superunit) are hosted by the Jánov Grúň complex, dated to Permian–Lower Triassic. Petro (1973) found veins that penetrated even into Jurassic rocks. Pršek et al. (2010) dated monazite from Bacúch; they mention "Permian and Alpine events" that were confirmed by the dating without giving more numerical or other details. Pršek & Chovan (2001) supposed that the siderite–quartz–sulfide veins extend continuously from Bacúch (in the Veporic Superunit) to Vyšná Boca (in the Tatric Superunit) across the tectonic boundary of the superunits, the Čertovica line. The basement elements of the Veporic Superunit and the southern Tatric complexes collided in the Late Turonian (≈90 Ma) (Putiš et al. 2009; Vojtko et al. 2017). If the veins truly pass through the tectonic boundary of the superunits, this datum would place an approximate upper limit on their age. The young age is also supported by the observation of Ferenc (2008) that similar siderite–quartz–sulfide veins pass across the tectonic boundary of the Veporic and Gemeric Superunits. Jacko & Baláž (1993) found that the quartz–siderite mineralisation in the Veporic rocks of Čierna hora Mts. occupies Upper Cretaceous tectonic structures but is crushed by post-Paleogene tectonics.

Further support for the young age of the siderite–ankerite–quartz–sulfide mineralisation is provided by the quartz–tourmaline stage, an integral part of many of these veins. In general, the quartz–tourmaline stage is prominently developed only in the Veporic Superunit which is the one most strongly affected by Alpine metamorphism. This stage is temporally sandwiched between the older siderite–ankerite and younger quartz–Cu-sulfide stages (Table 1). It consists of quartz, albite, schorl, apatite, zircon, and monazite and its extent at the known localities varies from prominent to almost negligible. Some of the monazite grains could be chemically (CHIME) dated. The age of monazite from Kolba (Veporic Superunit) was determined as 92±11 Ma, two samples from Jedľové Kostoľany (Tatric Superunit) gave 83±9 and 121±24 Ma (Chovan et al. 2006). These data agree with an earlier estimate of 90–140 Ma, derived from K/Ar dating of adularia (Hurai et al. 1991), combined with models of cooling and exhumation of the Veporic basement. They also coincide with the K/Ar ages of illite from post-ore faults at the Kyslá deposit (108–110 Ma, Sasvári & Rozložník 1993), although a clear link between these two groups of ages is difficult to establish. The available geochronological data for the quartz–tourmaline stage are scattered and with large uncertainties. A grand average of these data is 100 Ma and this value will be used also in the text below. The uncertainty on this average is difficult to evaluate but one should keep in mind that the available data range from 74 (i.e., lower bound of 83±9) to 145 (upper bound of 121±24) Ma.

The only direct geochronological data that pertain to the quartz–Cu-sulfide stage could be the Ar/Ar dates for hydrothermal muscovite from Jedľové Kostoľany (Chovan et al. 2006). Muscovite formed here veinlets in carbonate–quartz–sulfide filling of the veins and gave ages of 75±1 and 75±2 Ma. These ages agree with the generally accepted observation that the quartz–Cu-sulfide stage is younger than the quartz–tourmaline stage.

Galena–sphalerite stage

The largest deposit that contains a prominent example of this stage is Soviansko. Majzlan et al. (2020) noted that although there is a number of other occurrences with galena and sphalerite, fluid inclusion studies (Majzlan et al. 2001; Luptáková 2007; Kubač et al. 2014) indicate that they may be mutually independent products of convergent processes that were able to mobilize and deposit lead and zinc. Hence, it is difficult to see these deposits and occurrences as a single group to which one age could be assigned.

Therefore, our work focuses only at the Soviansko deposit. The mineralisation here is dominated by dolomite–ankerite, followed by the quartz–tourmaline stage and finally the galena–sphalerite ores hosted by quartz. All attempts of U/Pb dating of the carbonates failed as they contain too much common lead. The quartz–tourmaline stage, with its rough age of 100 Ma (see above), provides an upper limit on the age of galena and sphalerite.

Ar/Ar dating of illite in the subsamples from alteration zones produced negative staircase patterns (Fig. 10), with rims older than the cores, and points at increased incorporation of excess ^{40}Ar from the percolating fluids. Such a process is not uncommon in alteration zones within an old basement. The maximum crystallisation age of the samples is therefore 96 Ma but even this value may be affected by excess Ar and their geologically relevant crystallisation age could be younger.

Additionally, both samples show a last high temperature step of distinctly higher age. It means that the samples contain a small portion of older micas which have grown under high temperature condition and release their Ar preferentially at high temperatures. These micas may be fragments from the country rock or overgrown cores from older alteration products. Due to the mixing of the gas components the age values from these last steps only indicate minimum ages. The geologically relevant ages from the older components could be much higher.

Hence, the Ar/Ar dating of illite from Soviansko can be seen as a confirmation of the geological observations on the temporal relationships among the mineralisation stages (Luptáková 2007). The quartz–tourmaline stage, bracketed at other localities to roughly 100 Ma, is postdated by the galena–sphalerite stage whose age is younger than 96 Ma.

Baryte and hematite stages

There are some geological constraints for the timing of the baryte and hematite stages. Baryte veins at Soviansko are younger than the minerals of the galena–sphalerite stage (Luptáková 2007) whose age was discussed in the previous paragraphs. Baryte veins are known to penetrate locally into the Lower Triassic sediments (e.g., at Trangoška, Turan 1961) or even into Middle Triassic rocks (Nižné Matejkovo). In the latter case, Pb/Pb dating of galena associated with baryte gave 235 Ma (Kohút 2002). Quartz–hematite veinlets are hosted by Lower Triassic sandstones or the crystalline basement. Hence, these mineralisations are younger than Lower Triassic. The quartz–hematite veinlets usually occur isolated, without any contact with the other hydrothermal stages. Ozdín & Chovan (1999) assert that the hematite veins represent the youngest mineralisation at Vyšná Boca.

Uranium mineralisation at Rišianka

In terms of mineralogy and ore textures, the U mineralisation at Rišianka deviates much from the uraninite pegmatite mineralisation at Dúbrava. Given the textures and the age determined in this work (sample RIŠ-3, 70±6 Ma), we assume that the U mineralisation at Rišianka is a product of remobilisation of sedimentary U-enrichment of Upper Permian age (Novotný & Badár 1971; Rojkovič 1980). This mineralisation is observed in a wide region of the north-eastern part of the Nízke Tatry Mts. in "red-beds" sediments. Typical constituents of the sedimentary ores are colloform uraninite, pyrite, marcasite, accompanied by copper sulfides and galena. Remobilisation of this U mineralisation in the Gemeric Superunit was documented in the Middle Cretaceous (Rojkovič et al. 1993; Rojkovič & Konečný 2005) or Late Triassic times (Demko et al. 2012; Števko et al. 2014).

The sample RIŠ-12, used for the U/Pb LA–SF–ICP–MS dating, gave a large scatter of possible ages (Fig. 7b), thus documenting the long and protracted history of repeated hydrothermal and tectonic events in the veins at Rišianka. A detailed study of the nearby occurrence Kľačianka (Fig. 1) confirmed multiple episodes of sulfosalt deposition (Hovorič 2008), some of them chemically akin to the quartz–Cu-sulfide stage (cf. Majzlan et al. 2020). In addition, the small region with the Rišianka and Kľačianka occurrences (Fig. 1) lies squeezed between the large Dúbrava and Magurka deposits. The principal vein direction at these deposits is fundamentally different (N–S at Dúbrava, E–W at Magurka). Mineralogical similarities suggest that the large deposits and the small occurrences were formed from the same or similar fluids and perhaps at the same time, meaning that there must have been a significant tectonic and deformational mismatch between the two large deposits, focused in the area of the Rišianka and Kľačianka occurrences. Such tectonic predisposition was then used by fluids of different origin to remobilize sulfides (Fig. 11a), carbonates (Fig. 7b), and the pre-existing uranium mineralisation.

Hence, we assume that young sulfosalts observed in our sample (RIŠ-3, see Fig. 11a) belong to one of the later remobilisation and re-deposition events of sulfide minerals, and not to the older stibnite–sphalerite–Pb–Sb-sulfosalts stage.

Timing of the studied Variscan mineralisations

The molybdenite stage appears to be closely related to the Variscan metamorphic and igneous activity. The Re/Os age of the late-magmatic or hydrothermal molybdenite (352–343 Ma, Table 4) compare well to the U/Pb age of

magmatic zircons (353±3 Ma, 344±3 Ma, 340±3 Ma and/or 330±10 Ma, Poller et al. 2001; Putiš et al. 2003; Broska et al. 2013; Kohút, unpublished data). Given that the textural evidence places the scheelite stage without doubt before the arsenopyrite–pyrite–gold stage at Dúbrava (Chovan et al. 1994), the biotite K/Ar cooling age of 330 Ma could correspond to scheelite formation or, perhaps more likely, remobilisation. There are signs of other episodes of remobilisation of the scheelite mineralisation during the late Variscan time.

Our results suggest that the arsenopyrite–pyrite–gold and stibnite–sphalerite–Pb–Sb-sulfosalts stages are temporally close, of late Variscan age, and represent perhaps a product of a single prolonged episode of fluid circulation and mineral deposition. Fluids of the arsenopyrite–pyrite–gold stage were aqueous, CO_2-rich, with low salinity (Chovan et al. 1995a). Fluid inclusion studies (Chovan et al. 1995a), arsenopyrite thermometry (Sachan & Chovan 1991), and chlorite thermometry from the high-temperature alteration features (Orvošová et al. 1998) converge at relatively high temperatures of 300–450 °C. These data for the age and temperature of deposition agree broadly with Ar/Ar ages of muscovite from a granitic orthogneiss from Bystrá dolina (332±1 Ma, Dallmeyer et al. 1996) and thermal modeling of the Variscan crust (Západné Tatry Mts, Moussallam et al. 2012) that showed rapid cooling of the magmatic–metamorphic complexes to temperatures around 400 °C at ≈330 Ma.

Fluid inclusions in stibnite (Chovan et al. 2010) are also aqueous, of low salinity, but devoid of CO_2, with homogenisation temperatures of 100–170 °C. In the light of the temporal similarity of these stages, it could be reasoned that the stibnite-depositing fluids were derived directly from the fluids responsible for the precipitation of pyrite, arsenopyrite, and gold, by simple cooling and CO_2 loss. Such fluid evolution would be also consistent with thermodynamic predictions (Williams-Jones & Normand 1997) which show that the solubility of antimony at temperatures above 250 °C is very high. Deposition of stibnite is principally controlled by temperature and commences usually at lower temperatures.

Our data show no record of Permian hydrothermal activity, even though Permian magmatic activity is well documented in the Western Carpathians, for example in lamprophyre dykes in the Tatric Superunit (e.g., Spišiak et al. 2018). With the exception of one single datum (sample K-13, 286±37 Ma) with a relatively large uncertainty, all other data in this sample set fall into Carboniferous.

Comparison of the Variscan mineralisations in Nízke Tatry Mts. and in alike tectonic units

In terms of age, our results agree well with the geochronology of the Au–Sb deposits in the adjacent Bohemian Massif. Němec & Zachariáš (2018) distinguished three types of Au–Sb deposits there. The main commodity of all of them is gold and only a few deposits possess moderate reserves of stibnite. The first group comprises large gold deposits (total estimated reserves 250–350 t of gold) with ages of 348–338 Ma (Zachariáš et al. 2001, 2013). The second type, with appreciable amount of stibnite, are not dated so well, but geological evidence narrows their possible age to 338–330 Ma (Němec & Zachariáš 2018). The third type is assumed to be of age of 300–290 Ma. Němec & Zachariáš (2018) also described two types of fluids – an earlier aqueous CO_2-rich fluid responsible for the formation of quartz veins with arsenopyrite, and a later aqueous fluid that precipitated stibnite and gold. A recent study of Ackerman et al. (2019) documented prolonged history of gold mineralisation in the Kašperské hory gold deposit between 341 and 325 Ma, with slow cooling of the Variscan magmatic and metamorphic complexes and the development of multiple mineralisation stages.

The ages reported for the Sb–Au mineralisation in the Bohemian Massif coincide with or postdate the ages found for similar mineralisations in the French Massif Central (Bouchot et al. 2005; Pochon et al. 2018). Tartèse et al. (2015, and references therein) determined an age range of 340–330 Ma for As–Sb–Pb mineralisation, using LA–ICP–MS dating of monazite overgrowth and geological arguments. Bouchot et al. (2005) assigned ages of 300–317 Ma, mostly from illite dating (K/Ar, Ar/Ar) or geological arguments. These ages correspond to the the main exhumation stage of the subducted continental crust, nappe stacking, and formation of inverted metamorphic sequences in the Armorican Massif (Ballèvre et al. 2009). Similar ages were also reported by gold mineralisations in the Iberian Massif and rationalised in terms of geological evolution of the European variscides by Romer & Kroner (2018).

Timing of the studied Mesozoic mineralisations

Our data show multiple episodes of hydrothermal and tectonic activity throughout Mesozoic and Tertiary (Fig. 6). On the other hand, there are no indications of Permian mineralisations in our results, such as the inferred Permian age of the mineralogically comparable siderite veins in the Southern Alps (Martin et al. 2017).

Jurassic continental rifting (Plašienka 2018) is documented in scattered K/Ar ages of illite (210–170 Ma, Chovan et al. 2010, 2013) in shear zones. The relevance of these ages to a stage or stages of ore mineralisations is not clear.

Vigorous tectonic activity at 140–120 Ma is documented by Ar/Ar ages on sheet silicates from the Tatric and Veporic Superunits (Maluski et al. 1993). At this time, the Tatric basement was experiencing post-rift thermal relaxation (Králiková et al. 2016). The Ar/Ar ages of Alpine amphiboles in metapelitic and metabasic rocks of 115–105 Ma indicate a rapid onset of the Alpine metamorphism in the Veporic Superunit (see also Plašienka et al. 1999). Further data show cooling and exhumation already at 80–90 Ma (Plašienka et al. 1999) or 72–77 Ma (Janák et al. 2001). The oldest Alpine ages of ore mineralisations were assigned to the dolomite–baryte–tetrahedrite stage which is a component of large stibnite deposits (e.g., Dúbrava). The ages of this stage are roughly centred at 144 Ma.

The siderite–ankerite, quartz–tourmaline, and quartz–Cu-sulfides stages are regionally distributed in the Tatric, Veporic, and Gemeric Superunits of the CWC. The limited geochronological data are largely related to the quartz–tourmaline stage which frequently contains monazite or xenotime. U/Pb LA–SF–ICP–MS dating of siderite will be a subject of future work.

Hence, in general, the available data indicate that the quartz–tourmaline stage formed i) simultaneously in the Tatric and Veporic Superunits (or at least the existing data cannot distinguish between the timing of this stage between the two superunits), and ii) after the peak of the Alpine metamorphism in the Veporic Superunit (≈110 Ma, Plašienka et al. 1999).

The CHIME ages determined for the monazite of the quartz–tourmaline stage in the Tatric and Veporic Superunits are scattered and centred around 100 Ma. On the other hand, dating of monazite from the quartz–tourmaline stage in Rožňava-Nadabula (Gemeric Superunit, Hurai et al. 2015) gave an age of 139±1 Ma and monazite from the Čučma deposit gave ages of 120±9 and 76±12 Ma (CHIME dating, Hurai et al. 2006). Hurai et al. (2015) discussed the consistency of the CHIME and LA–ICP–MS dating on monazite grains and pointed out some discrepancies. Since the ages of the Tatric and Veporic Superunits were determined by CHIME dating, they should be revisited in the future. Hence, the formation of the quartz–tourmaline stage can be temporally correlated to the Alpine metamorphism, at least in the Veporic Superunit.

The data from this study and earlier publications document vigorous tectonic and hydrothermal activity in the Uppermost Cretaceous. This period appears to be the formation time of the U mineralisation in Rišianka (sample RIŠ-3, U/Pb, 70±6 Ma), muscovite assigned to the quartz–Cu-sulfide stage from Jedľové Kostoľany (75±2 Ma), and a single age datum for hydrothermal carbonates from Dúbrava (sample 52, U/Pb, 72±4 Ma, Fig. 7a). These ages coincide with the mylonitisation ages in the basement rocks of in the Tríbeč and Malá Fatra Mts in the Tatric Superunit (72±2 Ma, Kráľ et al. 2002; 72±3 Ma, Hók et al. 2000). Although the mylonitisation ages do not apply directly to the Nízke Tatry Mts., these authors note that the mylonitisation events could have operated on a larger scale and could be applied to the rocks of the Tatric Superunit as a whole. Similar ages (78.4–81.9 Ma) from the youngest structures in the Kyslá deposit (Nízke Tatry Mts) were reported by Sasvári & Rozložník (1993).

Timing of the studied Tertiary mineralisations

Oligocene–Miocene evolution of the CWC was also controlled by the north-western progression of the Alpine orogeny. The northern, frontal portions of CWC, buried previously under the Central Carpathian Paleogene Basin (CCPB), were undergoing exhumation (Králiková et al. 2014). The estimated loading of 4–7 km of Paleogene sediments in the Tatry Mts. caused a temperature increase up to 100–150 °C, peaking at 23 Ma. The youngest record in our hydrothermal carbonates are ages averaging at 24 Ma. Hence, the youngest remobilisation of the hydrothermal minerals can be linked to the tectonic burial of the Variscan cores in the Tatric Superunit. There is no evidence that this remobilisation brought new ore minerals, either in the Tatric or in the Veporic Superunits.

Comparison of the Alpine mineralisations in Nízke Tatry Mts. and in alike tectonic units

There are two types of regional siderite mineralisation in the eastern Alps, metasomatic and vein type (Prochaska 2016). Prochaska (2016) also discussed the long history of syngenetic and epigenetic models for this type of mineralisation and the tendency to accept the epigenetic views of the origin of these ores. Prochaska et al. (1996) reported Jurassic ages for this mineralisation (158±1, 147±1 Ma), based on Ar/Ar dating of alteration illite. They also reported a prominent remobilisation event, dated to ≈90 Ma and linked to Cretaceous metamorphism. Later, these ideas were revised in the light of Sm/Nd dating on the carbonates (Prochaska 2016) and it was argued that the mineralisation is Triassic (222–208 Ma). It should be also noted that these ages are also thought to be valid for the regional metasomatic magnesite mineralisation (Prochaska 2016) that is correlated with similar magnesite bodies in the Gemeric Superunit of the CWC.

In CWC, the vein type of siderite-ankerite mineralisation dominates in Tatric, Veporic, and Gemeric Superunits, with the largest deposits in the Gemeric Superunit (Rudňany, Rožňava, Rojkovič 1985; Grecula et al. 1995). Metasomatic siderite mineralisation is also known but it is less voluminous (e.g., Dobšiná, Mesarčík et al. 2001). The current knowledge of the siderite mineralisation in the CWC speaks against the temporal similarity with the Eastern Alps (Triassic) or the proposed Permian age of siderite (Radvanec & Grecula 2016). The geochronological and geological data in this work (Tatric Superunit) and the data from the Gemeric Superunit (Hurai et al. 2002, 2006, 2015) favor younger, Jurassic–Cretaceous age of the veins with siderite, ankerite, baryte, and sulfide minerals, mostly tetrahedrite and chalcopyrite.

Conclusions

The geochronological data collected and reviewed in this work identified a number of episodes of hydrothermal activity in Nízke Tatry Mts., related to other Variscan and Alpine complexes in the Tatric and Veporic Superunits. These episodes are related to:

- Variscan magmatic/high-grade metamorphic processes that generated uraninite crystals in pegmatite and quartz veinlets with molybdenite at 343–352 Ma, an age comparable to that of the host rocks;
- fluid circulation and cooling after the peak of the Variscan metamorphism that generated or remobilised scheelite ores (330 Ma) and generated the arsenopyrite–pyrite–gold (320 Ma) and stibnite–sphalerite–Pb–Sb-sulfosalts (320 Ma) stages;

- Jurassic continental rifting, shown by scattered K/Ar ages of illite from the Variscan basement cores;
- post-rift thermal relaxation of the Tatric basement and the formation of the dolomite–baryte–tetrahedrite stage, with the geochronological data averaging to ≈144 Ma;
- mid-Cretaceous Alpine metamorphism, prominent especially in the Veporic Superunit, accompanied by shortening, nappe stacking and formation of the quartz–tourmaline stage, with the scattered data averaging to ≈100 Ma;
- compression of the Tatric and Veporic complexes related to the subduction at the northern edge of the Western Carpathians, manifested by regional mylonitisation in the Tatric basement (72 Ma) and minor remobilisation of U minerals (70 Ma) and carbonates in ore veins (72 Ma). These events could be related to the formation of the quartz–Cu-sulfide stage (indirectly dated on muscovite, 75 Ma) and the galena–sphalerite stage (maximum age of 96 Ma);
- burial of parts of the Tatric basement under the Central Carpathian Paleogene Basin, seen as extensive remobilisation of vein carbonates (24 Ma);

Acknowledgements: We appreciate the constructive criticism of the reviewers I. Broska and T. Mikuš and the editorial handling by P. Koděra. This work was financially supported by the *Deutsche Forschungsgemeinschaft* grant KI 2131/2-1.

References

Ackerman L., Haluzová E., Creaser R.A., Pašava J., Veselovský F., Breiter K., Erban V. & Drábek M. 2017: Temporal evolution of mineralization events in the Bohemian Massif inferred from the Re–Os geochronology of molybdenite. *Miner. Deposita* 52, 651–662. https://doi.org/10.1007/s00126-016-0685-5

Ackerman L., Žák K., Haluzová E., Creaser R.A., Svojtka M., Pašava J. & Veselovský F. 2019: Chronology of the Kašperské Hory orogenic gold deposit, Bohemian Massif, Czech Republic. *Miner. Deposita* 54, 473–484. https://doi.org/10.1007/s00126-018-0822-4

Anczkiewicz A.A., Danišík M. & Środoń J. 2015: Multiple low-temperature thermochronology constraints on exhumation of the Tatra Mountains: New implication for the complex evolution of the Western Carpathians in the Cenozoic. *Tectonics* 34, 2296–2317. https://doi.org/10.1002/2015TC003952

Bagdasaryan G.P., Gukasyan R.Kh., Cambel B. & Veselský J. 1985: Rb-Sr isochron dating of the Ďumbier zone granitoids of the Nízke Tatry Mts. (Western Carpathians). *Geol. Zborn. Geol. Carpath.* 36, 637–645 (in Russian).

Bakos F., Chovan M. & Michálek J. 2000: Mineralogical composition of the hydrothermal Sb, Cu, Pb, Zn, As mineralization NE from Magurka in the Nízke Tatry Mts. *Miner. Slov.* 32, 497–506 (in Slovak).

Bakos F., Mikuš T., Biroň A. & Vavrová J. 2004: Hydrothermal Au mineralization in Harmanec (Starohorské vrchy Mts.). *Miner. Slov.* 36, 291–302 (in Slovak).

Ballèvre M., Bosse V., Ducassou C. & Pitra P. 2009: Palaeozoic history of the Armorican Massif: models for the tectonic evolution of the suture zones. *C.R. Geosci.* 341, 174–201. https://doi.org/10.1016/j.crte.2008.11.009

Balogh K., Ahijado A., Casillas R. & Fernandez C. 1999: Contributions to the chronology of the Basal Complex of Fuerteventura, Canary Islands. *J. Volcan. Geoth. Res.* 90, 81–101.

Biely A. (Ed.) 1992: Geological map of the Nízke Tatry Mts 1:50.000. *Dionýz Štúr Geol. Inst.,* Bratislava.

Bláha M. & Bartoň B. 1991: Jasenie W, Au, Jasenie-north. Final report – Mineralogy. *Open-file report, Geological Survey* Spišská Nová Ves, 1–64 (in Slovak).

Bouchot V., Ledru P., Lerouge C., Lescuyer J.L. & Milesi J.P. 2005: Late Variscan mineralizing systems related to orogenic processes: the French Massif Central. *Ore Geol. Rev.* 27, 169–197. https://doi.org/10.1016/j.oregeorev.2005.07.017

Broska I. & Kubiš M. 2018: Accessory minerals and evolution of tin-bearing S-type granites in the western segment of the Gemeric unit (Western Carpathians). *Geol. Carpath.* 69, 483–497. https://doi.org/10.1515/geoca-2018-0028

Broska I., Petrík I., Be'eri-Shlevin Y., Majka J. & Bezák V. 2013: Devonian/Mississippian I-type granitoids in the Western Carpathians: A subduction-related hybrid magmatism. *Lithos* 162, 27–36. https://doi.org/10.1016/j.lithos.2012.12.014

Burghele A. 1987: Propagation of error and choice of standard in the $^{40}Ar/^{39}Ar$ technique. *Chem. Geol.* 66, 17–19.

Chernyshev I., Cambel B. & Koděra M. 1984: Lead isotopes in galenas of the West Carpathians. *Geol. Carpath.* 35, 307–327.

Chovan M. 1981: Mineralogical and paragenetic investigation of the segment Matošovec (Dúbrava deposit). Manuskript. *Open File Report, Geofond*, Bratislava, 1–99 (in Slovak).

Chovan M., Háber M., Jeleň S. & Rojkovič I. (Eds.) 1994: Ore textures in the Western Carpathians. *Slovak Academic Press*, 1–219.

Chovan M., Hurai V., Sachan H.K. & Kantor J. 1995a: Origin of the fluids associated with granodiorite-hosted, Sb–As–Au–W mineralisation at Dúbrava (Nízke Tatry Mts., Western Carpathians). *Miner. Deposita* 30, 48–54.

Chovan M., Póč I., Jancsy P., Majzlan J. & Krištín J. 1995b: Sb–Au(As–Pb) mineralization of the deposit Magurka, Nízke Tatry Mts. *Miner. Slov.* 27, 397–406 (in Slovak).

Chovan M., Slavkay M. & Michálek J. 1996: Ore mineralizations of the Ďumbierske Tatry Mts. (Western Carpathians, Slovakia). *Geol. Carpath.* 47, 371–382.

Chovan M., Slavkay M. & Michálek J. 1998: Metallogenesis of the Ďumbier part of the Nízke Tatry Mts. *Miner. Slov.* 30, 3–8 (in Slovak).

Chovan M., Hurai V., Putiš M., Ozdín D., Pršek J., Moravanský D., Luptáková J., Záhradníková J., Kráľ J. & Konečný P. 2006: Fluid sources and formation of the mineralizations of the Tatric and northern Veporic units. *Open File Report, Comenius University*, Bratislava (in Slovak).

Chovan M., Hurai V., Lüders V., Prochaska W. & Balogh K. 2010: Origin of stibnite-bearing hydrothermal veins in the Tatric superunit, Western Carpathians. In: IMA Conference, Budapest, Hungary, Book of Abstracts, 231.

Chovan M., Konečný P., Putiš M., Jiang S.-Y. & Radvanec M. 2013: U–Pb, CHIME and Re–Os dating in the area of occurrence of molybdenite mineralization in the Nízke Tatry Mts. In: Book of Abstracts, MinPet conference (in Slovak).

Dallmeyer R.D., Neubauer F., Handler R., Fritz H., Müller W., Pana D. & Putiš M. 1996: Tectonothermal evolution of the internal Alps and Carpathians: Evidence from $^{40}Ar/^{39}Ar$ mineral and whole-rock data. *Eclogae Geol. Helv.* 89, 203–227.

Daniel J., Tulis J. & Čížek P. 1984: Report on geological and exploration work in 1983. *Uranium Exploration,* Spišská Nová Ves, 1–95 (in Slovak).

Danišík M., Kohút M., Dunkl I. & Frisch W. 2008: Thermal evolution of the Žiar Mountains basement (Inner Western Carpathians, Slovakia) constrained by fission track data. *Geol. Carpath.* 59, 19–30.

Danišík M., Kohút M., Broska I. & Frisch W. 2010: Thermal evolution of the Malá Fatra Mts. (Western Carpathians) - insights from zircon and apatite fission track thermochronology. *Geol. Carpath.* 61, 19–27.

Danišík M., Kadlec J., Glotzbach C., Weisheit A., Dunkl I., Kohút M., Evans N.J., Orvošová M. & McDonald B.J. 2011: Tracing metamorphism, exhumation and topographic evolution in orogenic belts by multiple thermochronology: a case study from the Nízke Tatry Mts., Western Carpathians. *Swiss J. Geosci.* 104, 285–298. https://doi.org/10.1007/s00015-011-0060-6

Dávidová Š. 1998: Granite pegmatite from the Dúbrava deposit in Nízke Tatry Mts – mineralogy and petrogenesis. *Miner. Slov.* 30, 36–43 (in Slovak).

Demko R., Ferenc Š., Biroň A., Novotný L. & Bartalský B. 2012: The genesis of the Kurišková U-Mo ore deposit. *Esemestník* 1, 24–25.

Eichhorn R., Schaerer U. & Höll R. 1995: Age and evolution of scheelite-hosting rocks in the Felbertal Deposit (Eastern Alps); U–Pb geochronology of zircon and titanite. *Contrib. Miner. Petrol.* 119, 377–386.

Ferenc Š. 2008: Metallogenetic aspects of the Alpine collision-extension zone of the Veporic unit (NW part). *PhD Thesis, Comenius University*, Bratislava, 1–162 (in Slovak).

Frimmel H.E. & Frank W. 1998: Neoproterozoic tectonothermal evolution of the Garieb Belt and its basement, Namibia and South Africa. *Precambrian Res.* 90, 1–28.

Gerdes A. & Zeh A. 2009: Zircon formation versus zircon alteration – New insights from combined U-Pb and Lu-Hf in-situ LA-ICP-MS analyses of Archean zircons from the Limpopo Belt. *Chem. Geol.* 261, 230–243. https://doi.org/10.1016/j.chemgeo.2008.03.005

Goldfarb R.J. & Groves D.I. 2015: Orogenic gold: Common or evolving fluid and metal sources through time. *Lithos* 233, 2–26. https://doi.org/10.1016/j.lithos.2015.07.011

Grathoff, G. & Moore, D.M. 1996: Illite polytype quantification using WILDFIRE© calculated X-Ray diffraction patterns. *Clays Clay Miner.* 44, 835–842.

Grecula P. 1971: Quartz vein deposits in Slovakia. *Miner. Slov.* 3, 349–370 (in Slovak).

Grecula P., Abonyi A., Abonyiová M., Antaš J., Bartalský B., Bartalský J., Dianiška I., Drnzík E., Ďuďa R., Gargulák M., Gazdačko Ľ., Hudáček J., Kobulský J., Lörincz L., Macko J., Návesňák D., Németh Z., Novotný L., Radvanec M., Rojkovič I., Rozložník L., Rozložník O., Varček C. & Zlocha J. 1995: Mineral deposits of the Slovak Ore Mountains. *Geocomplex*, Bratislava.

Harman M. 1956: Geological and paragenetic relations of the NW part of the Dúbrava stibnite mineralization and a few remarks to ores in the Nízke Tatry Mts. *Geol. Práce, Zpr.* 6, 56–70 (in Slovak).

Hók J., Siman P., Frank W., Kráľ J., Kotulová J. & Rakús M. 2000: Origin and exhumation of mylonites in the Lúčanská Malá Fatra Mts., (the Western Carpathians). *Slovak Geol. Mag.* 6, 325–334.

Hovorič R. 2008: Description of Sb mineralization at the localities Malé Železné and Kľačianka. *Diploma Thesis, Comenius University*, Bratislava, 1–117 (in Slovak).

Hurai V., Dávidová Š. & Kantor J. 1991: Adularia from alpine fissures of the Veporicum crystalline complexes: morphology, physical and chemical properties, fluid inclusion and K/Ar dating. *Miner. Slov.* 23, 133–144.

Hurai V., Harčová E., Huraiová M., Ozdín D., Prochaska W. & Wiegerová V. 2002: Origin of siderite veins in the Western Carpathians I. P-T-X-$\delta^{13}C$-$\delta^{18}O$ relations in ore-forming brines of the Rudňany deposits. *Ore Geol. Rev.* 21, 67–101.

Hurai V., Urban M., Konečný P., Thomas R., Lexa O., Schulmann K. & Chovan M. 2006: Cretaceous age of quartz-stibnite veins near Čučma (Spišsko-gemerské rudohorie Mts). *Miner. Slov.* 38, 131–140.

Hurai V., Paquette L., Lexa O., Konečný P. & Dianiška I. 2015: U–Pb–Th geochronology of monazite and zircon in albitite metasomatites of the Rožňava-Nadabula ore field (Western Carpathians, Slovakia): Implications for the origin of hydrothermal polymetallic siderite veins. *Miner. Petrol.* 109. https://doi.org/10.1007/s00710-015-0389-z

Ilavský J. & Sattran V. 1976: An outline of the metallogenesis of Czechoslovakia. *Miner. Slov.* 8, 193–288 (in Slovak).

Jacko S. & Baláž B. 1993: New knowledge about the Čierna hora Mts. metallogenese (Western Carpathians). *Miner. Slov.* 25, 323–326.

Jackson M.L. 1975: Soil Chemical Analysis: Advanced Course. 2nd edition. Madison, 1–1790.

Jakeš P. 1963: Contribution to the understanding of the stibnite veins on the northwestern slope of the Nízke Tatry Mts in the area of the locality Dúbrava. *Acta Univ. Carol. Geol.* 3, 159–178.

Janák M., Plašienka D., Frey M., Cosca M., Schmidt T., Lupták B. & Méres Š. 2001: Cretaceous evolution of a metamorphic core complex, the Veporic unit, Western Carpathians (Slovakia); P-T conditions and in situ $^{40}Ar/^{39}Ar$ UV laser probe dating of metapelites. *J. Metam. Geol.* 19, 197–216. https://doi.org/10.1046/j.0263-4929.2000.00304.x

Jourdan F. & Renne P.R. 2007: Age calibration of the Fish Canyon sanidine $^{40}Ar/^{39}Ar$ dating standard using primary K-Ar standards. *Geochim. Cosmochim. Acta* 71, 387–402. https://doi.org/10.1016/j.gca.2006.09.002

Kantor J. & Eliáš K. 1983: Isotopic and paleothermic research. In: Pecho, J. (Ed.): Scheelite–gold mineralization in the Nízke Tatry Mts. Conferences, Symposia & Seminars, *Dionýz Štúr Geol. Inst.,* Bratislava, 85-96 (in Slovak).

Kohút M. 1998: Genetic aspects of the Nízke Tatry Mts granitic rocks genesis. *Miner. Slov.* 30, 83–84 (in Slovak).

Kohút M. 2002: The Hercynian granitic rocks - A possible source of the Western Carpathians crystalline basement metallogeny. *Miner. Slov.* 34, 1-18 (in Slovak with English summary).

Kohút M. 2004: The orthogneisses of the Western Carpathians: An overview. *Miner. Slov.* 36, 141-155 (in Slovak with English summary).

Kohút M. 2014: Granitic rocks – windows to crustal evolution during the Phanerozoic in the Western Carpathians. In: Beqiraj A. & Uta A. (Eds.): Proceedings XX Congress of the Carpathian–Balkan Geological Association, special issue, 2/2014, 192–195.

Kohút M. 2017: Reflects a bimodal distribution of the monazite ages from the Western Carpathians Hercynian granites some real geological processes? In: *PetroS-2017 Conference*, 19–20.

Koutek J. 1931: Etudes géologiques sur les Basses Tatras du nord-ouest. *Sbor. St. Geol. Ust. Čs. Rep.*, IX., 413–616.

Kráľ J., Hók J., Frank W., Siman P., Liščák P. & Jánová V. 2002: Shear deformation in granodiorite: Structural, $^{40}Ar/^{39}Ar$, and geotechnical data (Tríbeč Mts., Western Carpathians). *Slovak Geol. Mag.* 8, 235–346.

Kráľ J. & Štarková Dž. 1995: $^{40}Ar/^{39}Ar$ dating of selected minerals from the Tatric and Veporic units. *Open File Report, Geofond,* Bratislava, 75 p. (in Slovak)

Králiková S., Vojtko R., Sliva Ľ., Minár J., Fügenschuh B., Kováč M. & Hók J. 2014: Cretaceous-Quaternary tectonic evolution of the Tatra Mts (Western Carpathians): Constraints from structural, sedimentary, geomorphological, and fission track data. *Geol. Carpath.* 65, 307–326. https://doi.org/10.2478/geoca-2014-0021

Králiková S., Vojtko R., Hók J., Fügenschuh B. & Kováč M. 2016: Low-temperature constraints on the Alpine thermal evolution of the Western Carpathian basement rock complexes. *J. Struct. Geol.* 91, 144–160. https://doi.org/10.1016/j.jsg.2016.09.006

Kubač A., Chovan M., Ozdín D. & Pukančík L. 2014: Hydrothermal Pb-Zn polymetallic mineralization at the locality Marianka (Malé Karpaty Mts.), Slovak republic. *Bull. miner.-petrol. Odd. Nár. Muzea* 22, 56-67 (in Slovak).

Lukáčik E. 1981: Petrology of the Prašivá granite-granodiorite type from the western part of Nízke Tatry Mts pluton. *Mineral. Petrogr. Geochem. Metalogen*. 8, 121-142 (in Slovak with English summary).

Luptáková J. 2007: Hydrothermal Pb-Zn mineralization in the Tatric tectonic unit of the Western Carpathians. *PhD Thesis, Comenius University*, Bratislava, 1–201 (in Slovak).

Majzlan J., Chovan M. & Michálek J. 1998: Ore occurrences at Rišianka and Malé Železné – mineralogy and paragenesis. *Miner. Slov.* 30, 52–59 (in Slovak).

Majzlan J., Hurai V. & Chovan M. 2001: Fluid inclusion and mineralogical study on hydrothermal As–Au–Sb–Cu–Pb–Zn veins in the Mlynná dolina valley (Western Carpathians, Slovakia). *Geol. Carpath.* 52, 277–286.

Majzlan J., Chovan M., Hurai V. & Luptáková J. 2020: Hydrothermal mineralisation of the Tatric Superunit (Western Carpathians, Slovakia): I. A review of mineralogical, thermometry and isotope data. *Geol. Carpath.* 71, 85–112. https://doi.org/10.31577/GeolCarp.71.2.1

Maluski H., Rajlich P. & Matte P. 1993: ^{40}Ar-^{39}Ar dating of the Inner Carpathians Variscan basement and Alpine mylonitic overprinting. *Tectonophysics* 223, 313–337.

Markey R., Stein H., Hannah J., Zimmerman, A., Selby D. & Creaser R.A. 2007: Standardizing Re–Os geochronology: A new molybdenite Reference Material (Henderson, USA) and the stoichiometry of Os salts. *Chem. Geol.* 244, 74–87. https://doi.org/10.1016/j.chemgeo.2007.06.002

Martin S., Toffolo L., Moroni M., Montorfano C., Secco L., Agnini C., Nimis P. & Tumiati S. 2017: Siderite deposits in northern Italy: Early Permian to Early Triassic hydrothermalism in the Southern Alps. *Lithos* 284–285, 276–295. https://doi.org/10.1016/j.lithos.2017.04.002

Mesarčík I., Kilík J., Lörincz L., Čapo J., Bajtoš P., Lehoczký M., Gluch A. & Mesarčíková M. 2001: Complex evaluation of the abandoned deposit Dobšiná. *Dionýz Štúr Geol. Inst.,* Bratislava, 1–223 (in Slovak).

Michálek J. & Chovan M. 1998: Structural-geological and mineralogical evaluation of the Sb deposit Dúbrava. *Miner. Slov.* 30, 25–35 (in Slovak).

Michalenko J. 1959: Preliminary report on a molybdenite occurrence in muscovite pegmatites and aplitic granits from the Malá Železná valley in the Nízke Tatry Mts. *Geol. Práce, Zprávy* 16, 101–104 (in Slovak).

Michalenko J. 1960: Report on a molybdenite occurrence in muscovite pegmatites and aplitic granits from the Malá Železná valley in the Nízke Tatry Mts. *Čas. Miner. Geol.* 5, 68–70 (in Slovak).

Michalenko J. 1962: On paleoid age of the stibnite ore mineralization at the Dúbrava deposit on the northeastern slopes of the Nízke Tatry Mts. *Geol. Práce, Zoš.* 62, 125–134 (in Slovak).

Mikulski S., Gaweda A. & Stein H.J. 2011: Re–Os age of molybdenite from the Tatra Mountains, Poland. *Mineral. Mag.* 75, 1470.

Molák B., Kantor J. & Bláha M. 1989: Biotite – possible indicator of the formation and age of the scheelite-gold ore mineralization in the area of Kyslá near Jasenie (Nízke Tatry Mts). In: Contributions to the seminar Scheelite mineralization in Czechoslovakia, 62–69.

Moore D.M. & Reynolds R.C.Jr. 1997: X-ray diffraction and the identification and analysis of clay minerals. *Oxford University Press*.

Moussallam Y., Scheider D.A., Janák M., Thöni M. & Holm D.K. 2012: Heterogeneous extrusion and exhumation of deep-crustal Variscan assembly: Geochronology of the Western Tatra Mountains, northern Slovakia. *Lithos* 144–145, 88–108.

Němec M. & Zachariáš J. 2018: The Krásná Hora, Milešov, and Příčovy Sb–Au ore deposits, Bohemian Massif: mineralogy, fluid inclusions, and stable isotope constraints on the deposit formation. *Miner. Deposita* 53, 225–244. https://doi.org/10.1007/s00126-017-0734-8

Novotný L. & Badár J. 1971: Stratigraphy, sedimentology and ore mineralization of the Lower Paleozoic of the Choč unit in the northeastern part of the Nízke Tatry Mts. *Miner. Slov.* 3, 23–41 (in Slovak).

Orvošová M., Majzlan J. & Chovan M. 1998: Hydrothermal alteration of granitoid rocks and gneisses in the Dúbrava Sb-Au deposit, Western Carpathians. *Geol. Carpath.* 49, 377–387.

Ozdín D. & Chovan M. 1999: New mineralogical and paragenetic knowledge about siderite veins in the vicinity of Vyšná Boca, Nízke Tatry Mts. *Slov. Geol. Mag.* 5, 255–271.

Paar W. & Köppel V. 1978: The ‚pitchblende-nodule-assemblage' of Mitterberg (Salzburg, Austria). *Neues Jahrb. Mineral. Abh.* 131, 254–271.

Petrík I. & Kohút M. 1997: The evolution of granitoid magmatism during the Hercynian orogen in the Western Carpathians. In: Grecula P., Hovorka D. & Putiš M. (Eds.): Geological evolution of the Western Carpathians. *Miner. Slov. Monograph,* 235–252.

Petro M. 1973: Mineral raw material at the sheet Polomka 1:25.000. *Open File Report, Geofond*, Bratislava (in Slovak).

Plašienka D. 2003: Development of basement-involved fold and thrust structures exemplified by the Tatric-Fatric-Veporic nappe system of the Western Carpathians (Slovakia). *Geodin. Acta* 16, 21–38. https://doi.org/10.1016/S0985-3111(02)00003-7

Plašienka D. 2018: Continuity and episodicity in the early Alpine tectonic evolution of the Western Carpathians: How large-scale processes are expressed by the orogenic architecture and rock record data. *Tectonics* 37, 2029–2079. https://doi.org/10.1029/2017TC004779

Plašienka D., Grecula P., Putiš M., Kováč M. & Hovorka D. 1997: Evolution and structure of the Western Carpathians: An overview. In: Grecula P., Hovorka D. & Putiš M. (eds): Geological evolution of the Western Carpathians. *Miner. Slov. Monograph*, 1–24.

Plašienka D., Janák M., Lupták B., Milovský R. & Frey M. 1999: Kinematics and metamorphism of Cretaceous core complex: the Veporic unit of the Western Carpathians. *Phys. Chem. Earth* 24, 651–658.

Pochon A., Gloaguen E., Branquet Y., Poujol M., Ruffet G., Boiron M.-C., Boulvais P., Gumiaux C., Cagnard F., Gouazou F. & Gapais D. 2018: Variscan Sb-Au mineralization in Central Brittany (France): A new metallogenic model derived from the Le Semnon district. *Ore Geol. Rev.* 97, 109–142. https://doi.org/10.1016/j.oregeorev.2018.04.016

Pouba Z. & Vejnar Z. 1955: Polymetallic ore veins near Jasenie in the Nízke Tatry Mts. *Sborník Ústř. Ústavu Geol., geol.* 485–556 (in Czech).

Polák M., Filo I., Havrila M., Bezák V., Kohút M., Kováč P., Vozár J., Mello J., Maglay J., Elečko M., Olšavský M., Pristaš J., Siman P., Buček S., Hók J., Rakús M., Lexa J. & Šimon L. 2003: Explanations to the geological map of the Starohorské Vrchy Mts, Čierťaž Mts and northern part of the Zvolenská kotlina depression in a scale 1:50.000. *Dionýz Štúr Publishing House*, 1–218 (in Slovak with English summary).

Poller U., Todt W., Kohút M. & Janák M. 2001: Nd, Sr, Pb isotope study of the Western Carpathians: implications for Palaeozoic evolution. *Schweiz. Mineralog. Petrograph. Mitt.* 81, 159–174.

Pouchou J.L. & Pichoir F. 1985: "PAP" (φρZ) procedure for improved quantitative microanalysis. In: Armstrong J.T. (Ed.): Microbeam Analysis. *San Francisco Press*, 104–106.

Prochaska W. 2016: Genetic concepts on the formation of the Austrian magnesite and siderite mineralizations in the Eastern Alps of Austria. *Geol. Croatica* 69, 31–38. https://doi.org/10.4154/GC.2016.03

Prochaska W., Frank W. & Bechtel A. 1996: Pretertiary siderite mineralization in the Greywacke Zone of the Eastern Alps. In: Grecula P. (Ed.): Variscan metallogeny in the Alpine orogenic belt. *Geokomplex*, Bratislava, 165–174.

Pršek J. & Chovan M. 2001: Hydrothermal carbonate and sulphide mineralization in the Late Paleozoic phyllites (Bacúch, Nízke Tatry Mts.). *Geolines* 13, 27–34.

Pršek J., Ondrejka M., Bačík P., Budzyń B. & Uher P. 2010: Metamorphic–hydrothermal REE minerals in the Bacúch magnetite deposit, Western Carpathians, Slovakia: (Sr,S)-rich monazite-(Ce) and Nd-dominant hingganite. *Can. Miner.* 48, 81–94. https://doi.org/10.3749/canmin.48.1.81

Putiš M., Kotov A.B., Petrík I., Korikovsky S.P., Madarás J., Salnikova E.B., Yakovleva S.Z., Berezhnaya N.G., Plotkina Y.V., Kovach V.P., Lupták B. & Majdán M. 2003: Early vs. late orogenic granitoids relationships in the Variscan basement of the Western Carpathians. *Geol. Carpath.* 54, 163–174.

Putiš M., Ivan P., Kohút M., Spišiak J., Siman P., Radvanec M., Uher P., Sergeev S., Larionov A., Méres Š., Demko R. & Ondrejka M. 2009: Meta-igneous rocks of the West-Carpathians basement as an indicator of Early Paleozoic extension-rifting/breakup events. *Bull. Soc. Géol. France* 180, 461–471.

Radvanec M. & Grecula P. 2016: Geotectonic and metallogenetic evolution of Gemericum (Inner Western Carpathians) from Ordovician to Jurassic. *Miner. Slov.* 48, 105–118.

Raith J.G. & Stein H.J. 2006: Variscan ore formation and metamorphism at the Felbertal scheelite deposit (Austria): constraining tungsten mineralisation from Re-Os dating of molybdenite. *Contrib. Mineral. Petrol.* 152, 505–521. https://doi.org/10.1007/s00410-006-0118-z

Renne P.R., Deino A.L., Walter R.C., Turrin B.D., Swisher C.C., Becker G.H., Curtis W.D., Sharo W.D. & Jaouni A.R. 1994: Intercalibration of astronomical and radioisotopic time. *Geology* 22, 783–786.

Roberts N.M.W., Rasbury E.T., Parrish R.R., Smith C.J., Horstwood M.S.A. & Condon D.J. 2017: A calcite reference material for LA-ICP-MS U-Pb geochronology. *Geochem. Geophy. Geosy.* https://doi.org/10.1002/2016GC006784

Rojkovič I. 1980: Uranium mineralization in the Permian of the Western Carpathians. In: Materialy XI. kongressa Karpato-Balkanskoj geologicheskoj associacii, sek. Mineralogiya i geochimiya. *Naukova Dumka*, Kyjev, 213-221.

Rojkovič I. 1985: Paragenesis and mineral succession. In: Cambel B. & Jarkovský J. (Eds.): The Rudňany Ore Field – Geochemical and Metalogenetic Characteristics. *Veda*, Bratislava, 183–193 (in Slovak).

Rojkovič I. & Konečný N. 2005: Th–U–Pb dating of monazite from the Cretaceous uranium vein mineralization in the Permian rocks of the Western Carpathians. *Geol. Carpath.* 56, 493–502.

Rojkovič I., Novotný L. & Háber M. 1993: Stratiform and vein U, Mo and Cu mineralization in the Novoveská Huta area, ČSFR. *Miner. Deposita* 28, 58–65.

Romer R.L. & Kroner U. 2018: Paleozoic gold in the Appalachians and Variscides. *Ore Geol. Rev.* 92, 475–505. https://doi.org/10.1016/j.oregeorev.2017.11.021

Sachan H.K. & Chovan M. 1991: Thermometry of arsenopyrite–pyrite mineralization in the Dúbrava antimony deposit (Western Carpathians). *Geol. Carpath.* 42, 265–269.

Sasvári T. & Rozložník L. 1993: Structural and metallogenetical presumptions of the scheelite metallogeny in the SE part of the L. Tatra Mts. *Miner. Slov.* 25, 320–322 (in Slovak).

Selby D. & Creaser R.A. 2001: Re–Os geochronology and systematics in molybdenite from the Endako porphyry molybdenum deposit, British Columbia, Canada. *Econ. Geol.* 96, 197–204. https://doi.org/10.2113/gsecongeo.96.1.197

Spišiak J., Vetráková L., Chew D., Ferenc Š., Mikuš T., Šimonová V. & Bačík P. 2018: Petrology and dating of the Permian lamprophyres from the Malá Fatra Mts. (Western Carpathians, Slovakia). *Geol. Carpath.* 69, 453–466. https://doi.org/10.1515/geoca-2018-0026

Środoń J. & Elsass F. 1994: Effect of the shape of fundamental particles on XRD characteristics of illitic minerals. *Eur. J. Miner.* 6, 113–122.

Steiger R.H. & Jäger E. 1977: Subcommission on geochronology: Convention on the use of decay constants in geo- and cosmochronology. *Earth Planet. Sci. Lett.* 36, 359–362.

Števko M., Uher P., Ondrejka M., Ozdín D. & Bačík P. 2014: Quartz–apatite–REE phosphates–uraninite vein mineralization near Čučma (eastern Slovakia): a product of early Alpine hydrothermal activity in the Gemeric Superunit, Western Carpathians. *J. Geosci.* 59, 209–222. https://doi.org/10.3190/jgeosci.169

Tartèse R., Poujol M., Gloaguen E., Boulvais P., Drost K., Košler J. & Ntaflos T. 2015: Hydrothermal activity during tectonic building of the Variscan orogen recorded by U-Pb systematics of xenotime in the Grès Armoricain formation, Massif Armoricain, France. *Miner. Petrol.* 109, 485–500. https://doi.org/10.1007/s00710-015-0373-7

Turan J. 1961: On the ores at Trangoška and about some occurrences in the valleys Bystrá and Mlynná on the southern slopes of the Nízke Tatry Mts. *Geol. Práce, Zprávy* 23, 85–114 (in Slovak).

Uher P., Kohút M. & Putiš M. 2011: Hercynian dioritic rocks of the Western Carpathians: tracers of crustal – mantle interactions. *Travaux géophys.* 40, 86.

Vojtko R., Králiková S., Andriessen P., Prokešová R., Minár J. & Jeřábek P. 2017: Geological evolution of the southwestern part of the Veporic Unit (Western Carpathians) based on fission track and morphotectonic data. *Geol. Carpath.* 68, 285–302. https://doi.org/10.1515/geoca-2017-0020

Waitzinger M. & Finger F. 2018: In-situ U–Th–Pb geochronometry with submicron-scale resolution: Low-voltage electron-beam dating of complexly zoned polygenetic uraninite microcrystals. *Geol. Carpath.* 69, 558–572. https://doi.org/10.1515/geoca-2018-0033

Williams-Jones A.E. & Normand C. 1997: Controls of mineral paragenesis in the system Fe-Sb-S-O. *Econ. Geol.* 92, 308–324.

Zachariáš J., Pertold Z., Pudilová M., Žák K., Pertoldová J., Stein H. & Markey R. 2001: Geology and genesis of Variscan porphyry-style gold mineralization, Petráčkova hora deposit, Bohemian Massif, Czech Republic. *Miner. Deposita* 36, 517–541. https://doi.org/10.1007/s001260100187

Zachariáš J., Žák K., Pudilová M. & Snee L.W. 2013: Multiple fluid sources/pathways and severe thermal gradients during formation of the Jílové orogenic gold deposit, Bohemian Massif, Czech Republic. *Ore Geol. Rev.* 54, 81–109. https://doi.org/10.1016/j.oregeorev.2013.02.012

Supplement

Table S1: Exact localisation and brief description of the samples used in this work.

Sample	Locality, brief description
uraninite	Dúbrava, Rakytová adit, crosscut PA-9/V. Pegmatite vein with pinkish feldspars, large muscovite flakes and uraninite crystals.
MŽ-1	Malé Železné, Vrchná František adit, near the face of the westward crosscut. Pegmatitic rock with minute molybdenite crystals.
602	Dúbrava, Lukáč adit, 50 m south from the point 333. Molybdenite in quartz veinlets, thickness up to 4 cm, in granodiorite.
814	Dúbrava, Rakytová adit, PA 9/V, 3 meters east from the point 183a. Hydrothermally altered granodiorite, with disseminated pyrite and arsenopyrite. In the vicinity several thin (up to 1 cm) quartz–stibnite veinlets
828	Dúbrava, Flotačná adit, P-1/V, 11 meters from the point 282, in the left-hand side of the drift. Hydrothermally altered granodiorite, with disseminated pyrite and arsenopyrite, in the vicinity of several thin (up to 1 cm) quartz–stibnite veinlets. Bulk Au analysis of the rock gave 9 ppm, gold is probably as invisible gold in arsenopyrite.
A-6a	Dúbrava, Flotačná adit, incline along the Dagmar vein, 6 m north from the point 143, granodiorite with strong hydrothermal alteration in the hanging wall of the vein.
A-10, A-11	Dúbrava, Rakytová adit, PA-9V, 7 meters from the point 192, granodiorite with strong hydrothermal alteration from the foot wall of the vein. A-10: 1 meter from the vein; A-11: at the contact of the vein and the country rock.
1A	Dúbrava, Flotačná adit, P-6, 26 meters east from the point 268, granodiorite with strong hydrothermal alteration from the hanging wall of the vein.
NASH – 19, 20	Pezinok-Cajla, Nová Alexander adit, samples of strongly hydrothermally altered granite.
1	Dúbrava, Flotačná adit, (FS4s, point 36) in the face, quartz–carbonate veinlets with sulfides and macroscopic zinkenite.
112a	Dúbrava, Svätopluk adit, section Matošovec, 36 meters south from the point 85. Side shoot of the Hlavná vein in a tectonic fracture in migmatites. Carbonate veinlet with massive and acicular stibnite.
52	Dúbrava, Svätopluk adit, 17 meters from the point 73, westward drift. A vein with N–S strike, composed of quartz, carbonate, stibnite, and pyrite.
K-13	Magurka, large dumps of the Kilian adit below the old mining road. Quartz–carbonate vein with stibnite.
302A	Dúbrava, Martin adit, HS 11j, in the face, 22 meters south from the point 244. Irregular vein swarm in strongly altered granite. The main vein is 11 cm thick, consists of quartz and pyrite at the contact with the country rock and Fe-dolomite and stibnite in the center. This vein is cut by a 1 cm thick carbonate veinlet, devoid of sulfides.
VS 10/4	Dúbrava, drill hole, depth 38 m, quartz–carbonate vein with stibnite.
131	Dúbrava, Flotačná adit, 6 meters south from the point 81, in the right-hand side of the drift. A quartz–pyrite vein is exposed over a length of 3 m. It contains tetrahedrite and is penetrated by less abundant carbonate. Thickness 20 cm, strike and dip 320/30 to E.
40	Dúbrava, Flotačná adit, 32 m from the point 52a. Up to 5 cm thick Fe-dolomite veinlet with small grains of tetrahedrite.
54	Dúbrava, Svätopluk adit, westward drift, 8 m from the point 73a. Vein with brecciated texture, fragments of altered rocks are cemented by quartz with coarse-grained carbonate with nests of tetrahedrite and chalcostibite.
125	Dúbrava, Svätopluk adit, 4 m east from the point 63, in the east crosscut in the ceiling. Younger carbonate veinlet with chalcostibite penetrates across a quartz–stibnite vein.
U-13	Dúbrava, Martin adit, 4 meters from the point 183. Migmatites and amphibole gneisses are strongly hydrothermally altered and host a stockwork of subparallel quartz–stibnite veinlets. These veinlets are cut by thin carbonates veinlets with scarce tetrahedrite.

Fig. S1. Photograph of the sample 1, used for dating in this work.

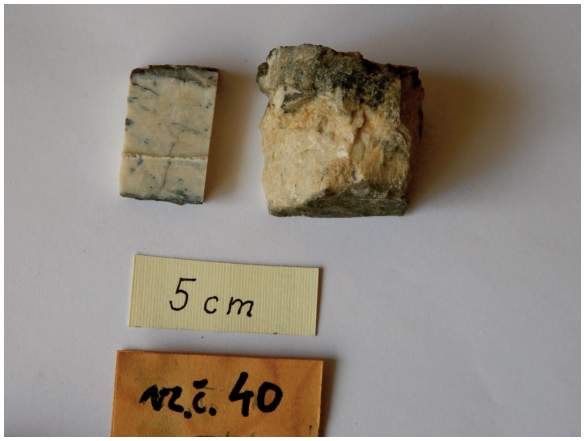

Fig. S2. Photograph of the sample 40, used for dating in this work.

Fig. S3. Photograph of the sample 52, used for dating in this work.

Fig. S4. Photograph of the sample 54, used for dating in this work.

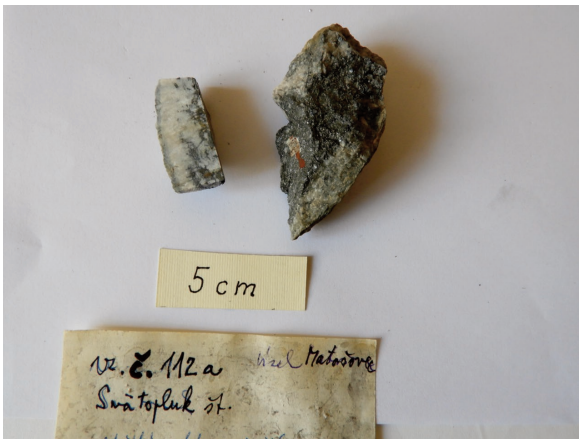

Fig. S5. Photograph of the sample 112a, used for dating in this work.

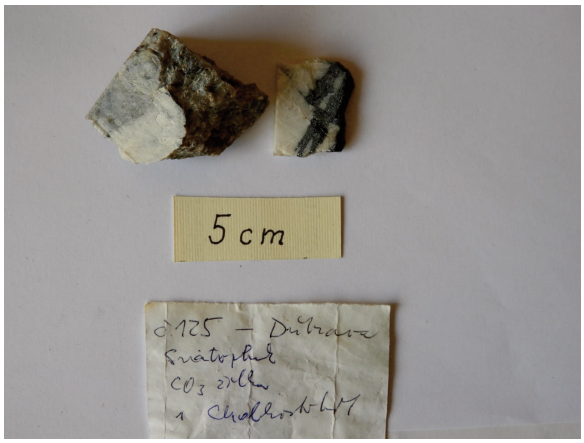

Fig. S6. Photograph of the sample 125, used for dating in this work.

Fig. S7. Two photographs of the sample 131, used for dating in this work.

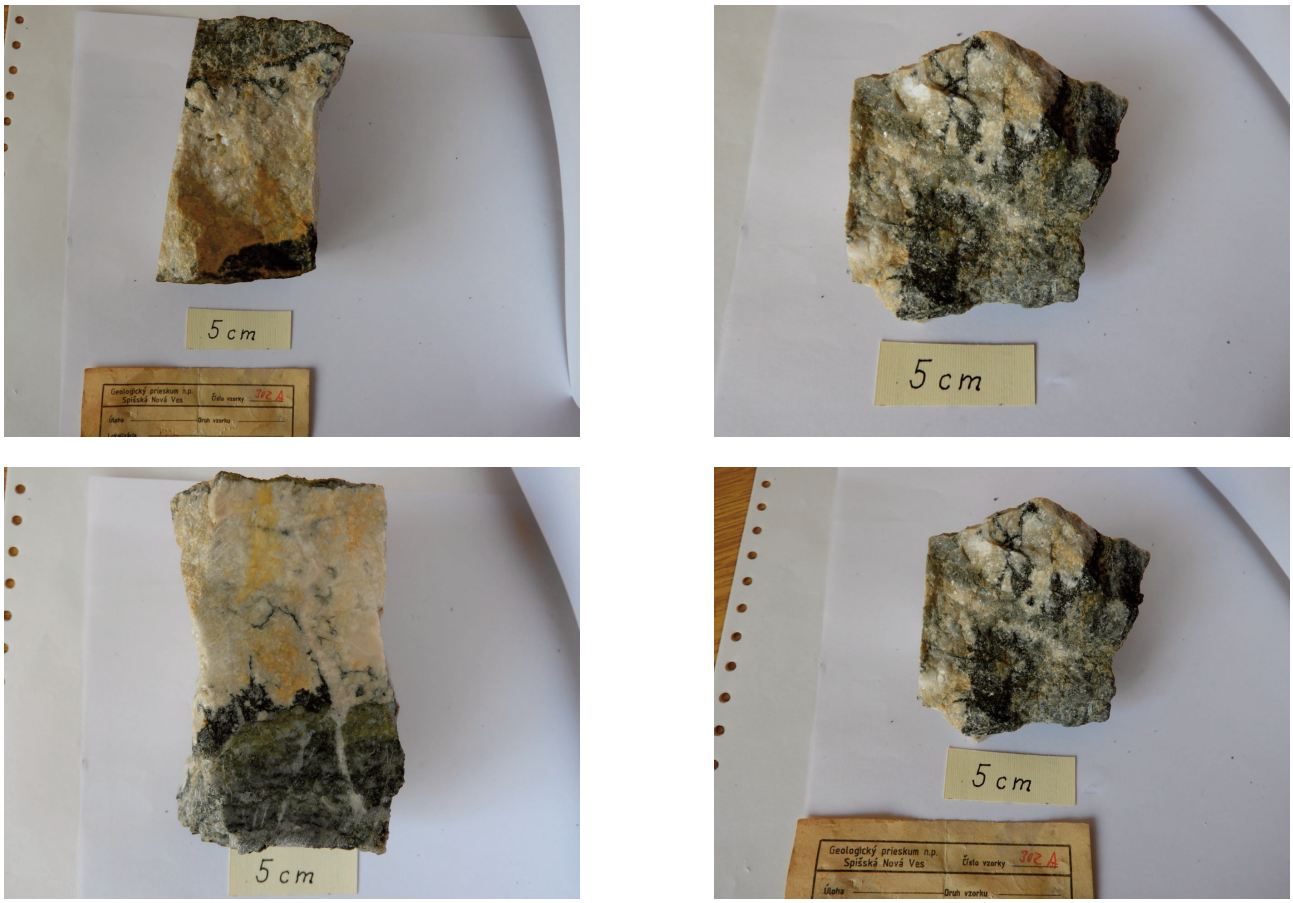

Fig. S8. Four photographs of the sample 302A, used for dating in this work.

Fig. S9. Photograph of the sample K-13, used for dating in this work.

Fig. S10. Photograph of the sample RIS-12, used for dating in this work.

Fig. S11. Photograph of the sample U-13, used for dating in this work.

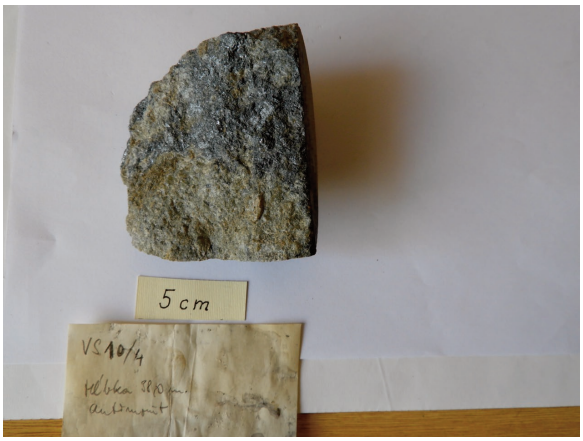

Fig. S12. Photograph of the sample VS10/4, used for dating in this work.

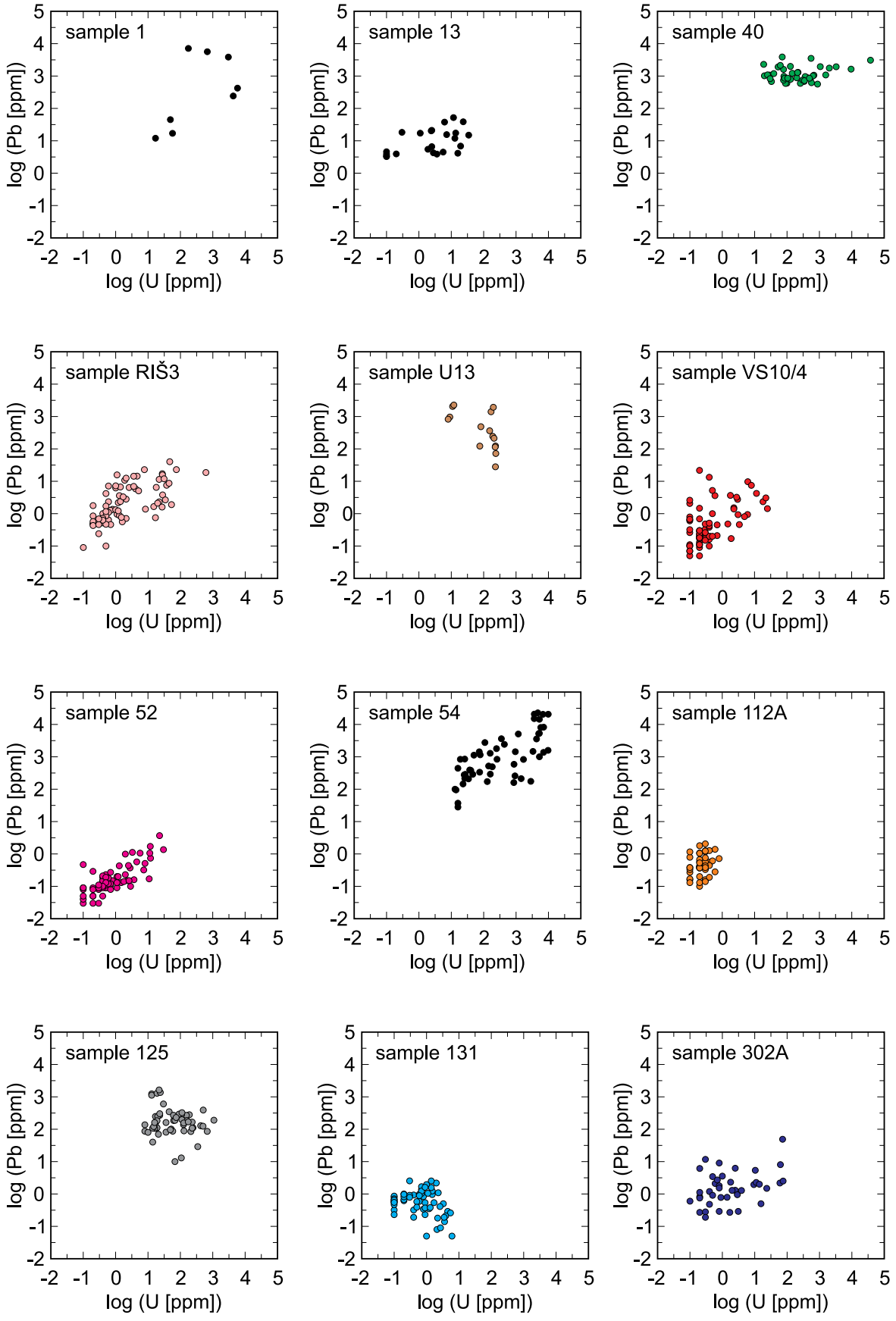

Fig. S13. Uranium and lead concentrations in individual spots in the samples used for dating in this work.

All samples were prepared in the form of polished and thin sections and examined in transmitted and reflected polarized light. Selected sections and minerals were further examined in an electron microprobe JEOL JXA-8230 (Jena) to obtain back-scattered electron (BSE) images, energy-dispersive (EDX) and wavelength-dispersive (WDX) analyses. The Pb–Sb sulfosalts (sample RIŠ-3, Table S2) were analyzed with and accelerating voltage of 20 kV, a beam current of 20 nA and a beam diameter of 1 μm. The elements and lines measured were Pb (Mα), Sb (Lα), Fe (Kα), Bi (Mα), S (Kα), Cu (Kα) and Zn (Kα) with counting times of 40 s. Overlap correction was performed to avoid peak interference between Fe and Pb as well as Fe and Bi. The standard specimens used for calibration were: galena for Pb, InSb for Sb, pyrite for Fe and S, Bi-metal for Bi, chalcopyrite for Cu and sphalerite for Zn. The detection limits, calculated from the peak and background counts, the measurement time, the beam current and the standard material concentration were: 0.3 wt. % for Pb, 0.07 wt. % for Sb, 0.04 wt. % for Fe, 0.1 wt. % for Bi, 0.02 wt. % for S, 0.05 wt. % for Cu and 0.06 wt. % for Zn.

Table S2: Electron microprobe analyses of Pb–Sb sulfosalts from Rišianka (sample RIŠ-3). Analytical results in wt. % are re-calculated to atomic %. The last column gives the Pb/Sb ratio (in at. %/at. %).

Point	Pb	Sb	Fe	Bi	S	Cu	Zn	Total	Pb	Sb	Fe	Bi	S	Cu	Zn	Pb/Sb
	wt.%								at.%							
1	36.41	42.8	0	0	20.34	0.01	0	99.56	15.13	30.26	0	0	54.6	0.02	0	0.4999
2	36.8	42.57	0.03	0	20.21	0	0.03	99.64	15.33	30.18	0.04	0	54.41	0	0.04	0.5081
3	36.94	42.52	0	0	20.31	0	0	99.77	15.36	30.08	0	0	54.55	0	0.01	0.5105
4	36.65	42.7	0.03	0	20.17	0	0.04	99.58	15.28	30.29	0.05	0	54.33	0	0.05	0.5044
5	36.65	42.69	0.01	0	20.25	0.01	0.01	99.61	15.26	30.24	0.02	0	54.46	0.01	0.01	0.5045
6	36.47	42.82	0	0	20.31	0	0.02	99.61	15.16	30.28	0	0	54.53	0	0.03	0.5006
7	36.84	42.6	0	0	20.25	0	0	99.69	15.34	30.18	0	0	54.48	0	0	0.5083
8	36.34	42.83	0.14	0	20.19	0	0	99.51	15.13	30.34	0.22	0	54.31	0	0	0.4986
9	36.6	42.73	0.01	0	20.27	0	0	99.61	15.23	30.26	0.02	0	54.5	0	0	0.5033
10	36.36	42.95	0	0	20.28	0.03	0	99.62	15.11	30.38	0	0	54.46	0.04	0	0.4974
11	37.31	42.15	0.03	0	20.13	0.02	0	99.63	15.6	29.98	0.04	0	54.36	0.03	0	0.5203
12	36.4	42.53	0.01	0	20.17	0	0.06	99.17	15.21	30.24	0.01	0	54.46	0	0.07	0.503
13	36.26	43.06	0.02	0	20.19	0	0.05	99.58	15.09	30.5	0.04	0	54.3	0	0.07	0.4948
14	36.64	42.55	0.02	0	20.07	0	0.03	99.31	15.34	30.31	0.02	0	54.28	0	0.04	0.506
15	39.15	42.19	0.18	0	20.31	0.04	0.04	101.91	16.1	29.53	0.27	0	53.99	0.05	0.05	0.5453
16	37.16	42.28	0.03	0	20.18	0.05	0.02	99.71	15.5	30.01	0.04	0	54.37	0.06	0.03	0.5165
17	36.49	42.64	0	0	20.13	0	0	99.26	15.26	30.35	0	0	54.39	0	0	0.5028
18	37.27	42.14	0.02	0	20.09	0.02	0.01	99.54	15.6	30.01	0.02	0	54.33	0.02	0.01	0.5196
19	36.94	42.21	0	0	20.11	0.03	0.03	99.31	15.46	30.06	0	0	54.4	0.03	0.05	0.5143
20	37.15	42.16	0.03	0	20.09	0.01	0.04	99.47	15.55	30.03	0.04	0	54.32	0.02	0.05	0.5178
21	36.89	42.84	0	0	19.98	0	0	99.71	15.44	30.52	0	0	54.04	0	0	0.506
22	36.95	42.42	0.01	0	20.13	0	0.03	99.55	15.43	30.16	0.02	0	54.34	0	0.04	0.5118
23	36.79	42.44	0	0	20.35	0	0	99.58	15.29	30.03	0	0	54.67	0	0	0.5093
24	37.31	42.24	0	0	20.16	0	0.01	99.72	15.58	30.02	0	0	54.4	0	0.01	0.519
25	36.5	42.76	0	0	20.14	0	0.01	99.4	15.24	30.39	0	0	54.36	0	0.01	0.5016
26	36.49	42.92	0	0	20.1	0.03	0	99.55	15.24	30.5	0	0	54.22	0.04	0	0.4996
27	36.73	42.56	0.04	0	20.13	0.02	0	99.47	15.34	30.25	0.07	0	54.32	0.03	0	0.5071
28	37.17	42.22	0.07	0	20.16	0	0.01	99.63	15.51	29.99	0.11	0	54.38	0	0.01	0.5173
29	37.28	42.2	0	0	19.5	0.01	0.06	99.05	15.84	30.52	0	0	53.54	0.02	0.08	0.519
30	38.33	41.62	0.01	0	19.24	0.03	0.01	99.24	16.4	30.31	0.02	0	53.21	0.04	0.01	0.5412
31	36.87	40.03	0.01	0	19.24	0.03	0.01	96.19	16.07	29.68	0.02	0	54.18	0.04	0.01	0.5412
32	36.15	43.3	0.01	0	19.92	0.01	0	99.39	15.15	30.87	0.02	0	53.94	0.02	0	0.4906
33	37.05	42.43	0	0	19.93	0	0.04	99.45	15.56	30.32	0	0	54.07	0	0.06	0.5131
34	36.04	43.28	0.01	0	20	0	0.01	99.34	15.08	30.82	0.01	0	54.08	0	0.02	0.4893
35	36.56	42.62	0.03	0	20.14	0	0	99.35	15.28	30.31	0.04	0	54.37	0	0	0.5041
36	37.1	42.31	0.04	0	20	0.02	0	99.48	15.55	30.18	0.07	0	54.17	0.03	0	0.5151
37	36.41	43.48	0.05	0	19.71	0.02	0.01	99.68	15.29	31.08	0.08	0	53.51	0.03	0.01	0.492
38	36.81	42.67	0.03	0	20.12	0.03	0	99.65	15.36	30.3	0.04	0	54.25	0.05	0	0.507
39	36.55	42.56	0.03	0	20.09	0	0.08	99.32	15.28	30.29	0.05	0	54.27	0	0.11	0.5047
40	36.62	42.81	0.06	0	19.91	0.02	0	99.42	15.36	30.56	0.1	0	53.95	0.03	0	0.5028

Table S2 (continued)

Point	Pb	Sb	Fe	Bi	S	Cu	Zn	Total	Pb	Sb	Fe	Bi	S	Cu	Zn	Pb/Sb
	wt.%								at.%							
41	36.86	42.49	0.06	0	20.13	0.03	0	99.56	15.39	30.19	0.1	0	54.29	0.04	0	0.5097
42	36.14	42.95	0	0	20.25	0	0	99.34	15.05	30.44	0	0	54.5	0	0	0.4945
43	36.29	43	0.03	0	20.07	0	0.05	99.44	15.16	30.57	0.05	0	54.16	0	0.07	0.4958
44	36.53	42.64	0.04	0	20.15	0.04	0.05	99.46	15.24	30.26	0.07	0	54.31	0.05	0.07	0.5035
45	36.52	42.67	0	0	20.28	0	0	99.47	15.21	30.23	0	0	54.56	0	0	0.503
46	36.27	43.13	0	0	19.88	0	0.04	99.32	15.23	30.81	0	0	53.91	0	0.05	0.4942
47	36.81	42.84	0	0	19.99	0	0.05	99.68	15.4	30.5	0	0	54.03	0	0.07	0.505
48	37.16	42.58	0	0	19.95	0	0.06	99.74	15.57	30.35	0	0	54	0	0.08	0.5128
49	36.79	42.57	0.01	0	20.06	0	0.01	99.44	15.4	30.32	0.02	0	54.25	0	0.02	0.5079
50	36.18	43.06	0.01	0	20.21	0	0	99.46	15.07	30.52	0.01	0	54.4	0	0	0.4938